Journal of Medicinal Chemistry

Article

Cite This: J. Med. Chem. XXXX, XXX, XXX−XXX

pubs.acs.org/jmc

Coupling of an Acyl Migration Prodrug Strategy with Bio-activation To Improve Oral Delivery of the HIV-1 Protease Inhibitor Atazanavir

Murugaiah A. M. Subbaiah,*[,†] Nicholas A. Meanwell,[‡] John F. Kadow,[‡,⊗] Lakshumanan Subramani,[†] Mathiazhagan Annadurai,[†] Thangeswaran Ramar,[†] Salil D. Desai,[§] Sarmistha Sinha,[⊥] Murali Subramanian,[⊥] Sandhya Mandlekar,[⊥] Srikanth Sridhar,[§] Shweta Padmanabhan,[⊥] Priyadeep Bhutani,[⊥] Rambabu Arla,[⊥] Susan M. Jenkins,[#,⊗] Mark R. Krystal,[∥,⊗] Chunfu X. Wang,[∥,⊗] and Ramakanth Sarabu[†]

Departments of [†]Medicinal Chemistry, [§]Biopharmaceutics, and [⊥]Pharmaceutical Candidate Optimization, Biocon-Bristol Myers Squibb R&D Centre, Biocon Park, Bommasandra IV Phase, Jigani Link Road, Bangalore 560099, India

Departments of [‡]Discovery Chemistry and Molecular Technologies, [∥]Virology, and [#]Pharmaceutical Candidate Optimization, Bristol-Myers Squibb Research and Development, 5 Research Parkway, Wallingford, Connecticut 06924, United States

Supporting Information

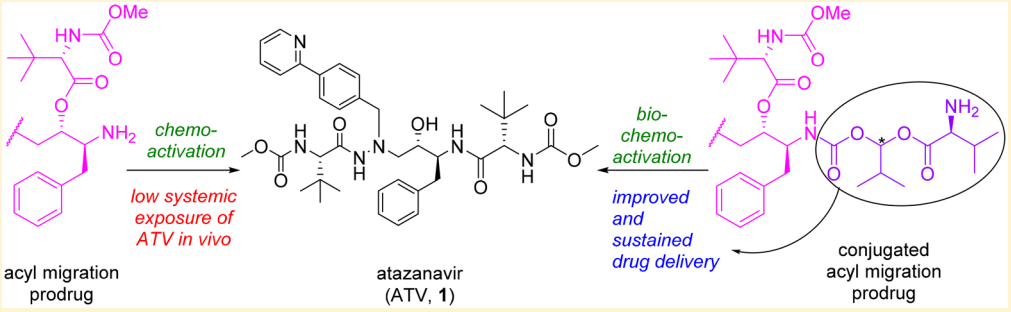

ABSTRACT: HIV-1 protease inhibitors (PIs), which include atazanavir (ATV, **1**), remain important medicines to treat HIV-1 infection. However, they are characterized by poor oral bioavailability and a need for boosting with a pharmacokinetic enhancer, which results in additional drug−drug interactions that are sometimes difficult to manage. We investigated a chemo-activated, acyl migration-based prodrug design approach to improve the pharmacokinetic profile of **1** but failed to obtain improved oral bioavailability over dosing the parent drug in rats. This strategy was refined by conjugating the amine with a promoiety designed to undergo bio-activation, as a means of modulating the subsequent chemo-activation. This culminated in a lead prodrug that (1) yielded substantially better oral drug delivery of **1** when compared to the parent itself, the simple acyl migration-based prodrug, and the corresponding simple L-Val prodrug, (2) acted as a depot which resulted in a sustained release of the parent drug in vivo, and (3) offered the benefit of mitigating the pH-dependent absorption associated with **1**, thereby potentially reducing the risk of decreased bioavailability with concurrent use of stomach-acid-reducing drugs.

INTRODUCTION

Combination antiretroviral therapy (cART), which is presently the most effective treatment for AIDS, has made it possible for HIV-1-infected patients to enjoy a high quality of life with a significant extension of life expectancy.[1,2] HIV-1 protease inhibitors (PIs) enabled cART and became a key component of drug combinations because of their robust efficacy, durability in treatment-naïve patients, and high genetic barrier to resistance development.[3,4] As a class, PIs are known for sub-optimal physicochemical and ADME properties, which contribute to poor oral bioavailability. This frequently demands high doses of the active drug and in most cases requires co-dosing with a pharmacokinetic (PK) enhancer in order to effectively deliver PIs. The resultant drug−drug interactions and related toxicities contribute to reduced patient compliance and limit the potential for the development of fixed-dose drug combinations (Figure 1).

Atazanavir (ATV, **1**), an azapeptide-based PI, was the first once-daily PI to be approved and has been included in the WHO's list of essential medicines.[5,6] **1** is marketed alone or in combination with the PK enhancers ritonavir or cobicistat.[7] **1** is characterized by sub-optimal oral bioavailability, which can be attributed to poor solubility at higher pH, high efflux,[8] and extensive first-pass metabolism. As a consequence of the solubility limitation, co-administration of **1** + ritonavir with the proton pump inhibitor (PPI) omeprazole leads to a 75% reduction in the exposure of **1**, indicative of pH-dependent absorption.[9,10] **1** requires clinical co-administration with a PK

Received: February 21, 2018

DOI: 10.1021/acs.jmedchem.8b00277
J. Med. Chem. XXXX, XXX, XXX−XXX

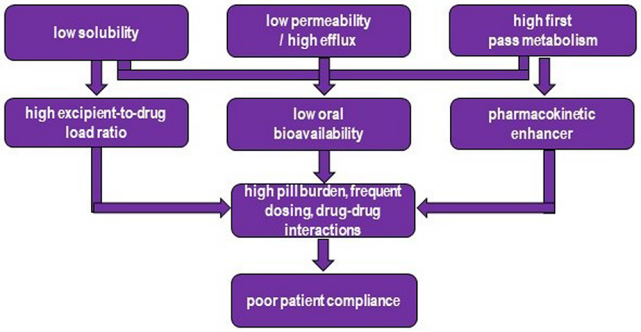

Figure 1. Reduced patient compliance as an outcome of poor oral bioavailability of PIs. Adapted with permission from ref 11.

enhancer that inhibits CYP3A metabolism, affording higher oral bioavailability, a longer plasma $t_{1/2}$, and a higher C_{trough} than that of unboosted **1**.

Attempts have been made to develop next-generation PIs that would exhibit improved pharmacokinetic, resistance, and/or safety profiles.[3,4] As an example, a deuterated version of **1**, D_{24}-ATV, has been investigated in an effort to enhance metabolic stability by taking advantage of the kinetic isotope effect to slow metabolism.[12] However, D_{24}-ATV exhibited only a modest improvement in plasma exposure in rats compared to **1**. Moreover, this approach does not address the pH-dependent absorption observed with **1**. There has been a growing interest in the exploration of prodrugs across all therapeutic classes, and a well-designed prodrug of **1** has the potential to address both its pharmaceutical and pharmacokinetic limitations.[13,14] Different prodrug approaches have been investigated in the literature to improve the ADME properties of the PIs, although none have been applied to **1**.[11,15,16] Phosphate prodrugs of the PIs lopinavir, ritonavir, and amprenavir have been explored in an effort to address dissolution-limited absorption and/or high load of solubilizing excipients, which led to the discovery of the marketed agent, fosamprenavir.[17,18] Amino acid and dipeptide prodrugs have been shown to improve absorptive permeability by the combined effect of active transport and decreased efflux and to reduce susceptibility to first-pass metabolism.[19−21] Peptide-based prodrugs of an analogue of darunavir that are designed to be activated by the ubiquitous dipeptidyl peptidase-IV enzyme have also been reported.[22] In addition to proton-coupled peptide transporter 1 (PepT1)-mediated transport of amino acid-based prodrugs, other prodrug strategies have been designed to take advantage of carrier-mediated transport and include, for example, ascorbic acid-conjugated prodrugs for targeting the sodium-dependent vitamin C transporter (SVCT),[23] biotin-derived prodrugs for targeting the sodium-dependent multivitamin transporter (SMVT),[24] and monocarboxylate ester prodrugs to target the fatty acid transport proteins (FATPs)[25] for placental delivery. Acyl migration prodrugs, which were designed to undergo pH-dependent activation and improve aqueous solubility, have also been explored.[26,27]

RESULTS AND DISCUSSION

We report herein the design of a novel double prodrug of **1** that relies upon sequential enzyme-mediated release of an amine that is designed to undergo an acyl migration to deliver the parent drug that (i) enables superior exposure based on improved pharmaceutical properties and a sustained release *in vivo* and (ii) attenuates the pH-dependent absorption of **1**. This design approach was found to be essential because simple prodrugs like the L-Val derivative **3** (Scheme 1) that were based on appending solubilizing elements to the secondary alcohol of **1** were unsuccessful at improving oral bioavailability, with the predominant circulation of prodrug itself.[11] This result prompted an examination of a design approach based on an *O*-to-*N* acyl migration concept that potentially offers the advantage of facile conversion of prodrug and higher atom economy which arises from the rearrangement of the prodrug to the parent without the release of a promoiety (Scheme 2).[26] This traceless prodrug strategy eliminates the release of a promoiety byproduct *in vivo*, reducing the potential for the introduction of additional toxicities.

Scheme 1. Synthesis of Direct L-Val Ester 3[a]

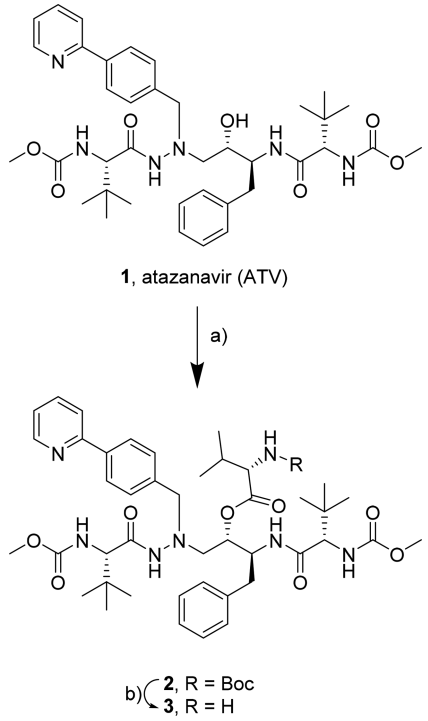

[a]Reagents and conditions: (a) *N*-Boc-L-Val, DCC, DMAP, DCM, RT, 12 h, 74.1%; (b) 4 N HCl in diethyl ether, 0 °C, 1 h, 85%.

The acyl migration prodrug **4** was retrosynthetically designed to release **1** by the chemical process depicted in Scheme 2. Prodrug **4** was synthesized in two steps from **5**, an intermediate in the synthesis of **1**,[28] as delineated in Scheme 3. *O*-Acylation of **5** with *N*-(methoxycarbonyl)-*tert*-L-leucine **6** followed by deprotection of the *N*-Boc group using 4 N HCl in dioxane afforded the amine **4** as the HCl salt. The intermediate **6** was prepared in one step from L-*tert*-leucine on treatment with methyl chloroformate following the literature protocol.[29] Prodrug **4** showed decreasing solution stability with increasing pH, with excellent stability at pH 1 and 4 ($t_{1/2}$ > 334 h) and lower stability at pH 6.5 ($t_{1/2}$ = 6.6 h); data are compiled in Table 1. Cognizant of solubility considerations associated with **1**, stability studies were performed in 30% aqueous acetonitrile. Consequently, the stability of **4** in a 100% aqueous system is expected to be lower than the $t_{1/2}$ of 6.6 h at pH 6.5 determined in the mixed solvent system. The low stability of **4** at pH 6.5 was anticipated based on the design strategy which relies upon rearrangement to **1** after amine deprotonation. Prodrug **4**

DOI: 10.1021/acs.jmedchem.8b00277
J. Med. Chem. XXXX, XXX, XXX−XXX

Scheme 2. Chemoactivable Prodrug Design Based on an *O*-to-*N* Acyl Migration[a]

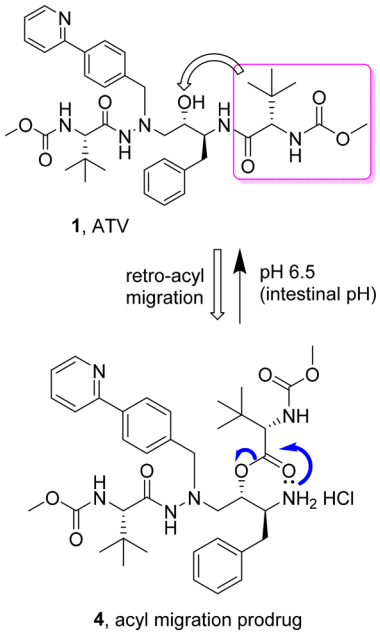

[a]Retrosynthetic design of a traceless acyl migration-based prodrug involving the transfer of the *tert*-leucine unit to the proximal secondary alcohol moiety.

Scheme 3. Synthesis of Acyl Migration Prodrug 4[a]

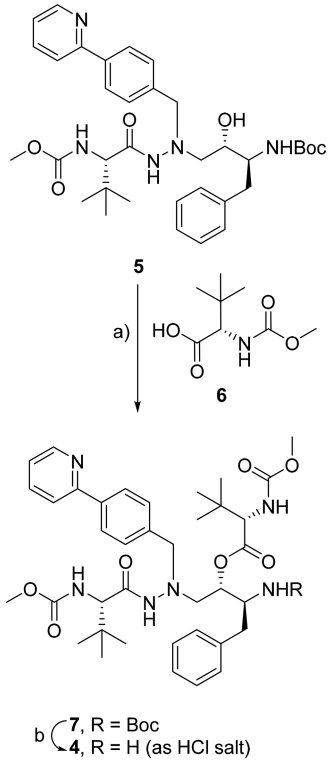

[a]Reagents and conditions: (a) intermediate **6**, DCC, DMAP, DCM, RT, 12 h, 52.5%; (b) 4 N HCl in dioxane, 0 °C, 1 h, 87%.

exhibited good aqueous solubility at pH 1 and 4 (>0.4 mg/mL), but solubility was not determined at pH 6.5 due to the short half-life of the prodrug at this pH. The *in vitro* profile of **4** suggests that the prodrug will be adequately stable in the stomach but will begin to release the parent after reaching the intestine. The prodrug was evaluated in Sprague–Dawley (SD) rats following oral administration at a dose of 3 mg/kg using a precipitation-resistant formulation to avoid any potential impact of dissolution on the exposure. Disappointingly, the exposure of **1** in this experiment was lower (relative F = 1%) when compared to the exposure obtained from a solution formulation of **1** (F = 20%) (Table 2 and Figure 2b). The trough concentration of the parent, obtained following administration of the prodrug, was also below the limit of quantification (BLQ).

Table 1. Stability and Solubility for 1 and Prodrugs[a]

	stability ($t_{1/2}$, h) at 37 °C			solubility (mg/mL) at 25 °C		
parent/prodrug	pH 1.0	pH 4.0	pH 6.5	pH 1.0	pH 4.0	pH 6.5
1	>500	>500	>500	1.69	<0.001	<0.001
4	376.4	334.3	6.6	>0.9	>0.4	ND
9	>500	>500	120.4	>1.8	<0.001	<0.001
11[b]	>500	334.3	6.6	>1.8	>1.5	ND
14	>500	>500	107.5	>1.1	0.12	0.01
16	>500	>500	214.9	>0.5	>1.43	0.027

[a]Stability studies used 30% acetonitrile in buffer. Buffers used were 0.1 N aqueous HCl (pH 1.0), acetate buffer (pH 4.0), and phosphate buffer (pH 6.5) at a concentration of 50 mM. ND = not determined. [b]Stability $t_{1/2}$ = 1.8 h at pH 7.4.

Following poor *in vivo* exposure of **1** from **4**, attention was focused on masking the amine of the acyl migration prodrug **4** through conjugation with an enzyme-releasable promoiety. The objectives were to improve solution stability at pH 6.5 and enable absorption of the intact prodrug, with enzyme-mediated cleavage of the prodrug occurring post-absorption. To the best of our knowledge, this approach does not have precedent in the literature. The criteria for choosing the promoiety were that it should (a) retain a polar, solubility-enhancing element and (b) also facilitate intestinal permeability through either passive diffusion or active transport. Contrary to the traceless nature of the acyl migration prodrug **4**, the conjugative acyl migration prodrugs are expected to release byproducts *in vivo*. Hence, the design elements should incorporate safety considerations that the released promoiety or byproduct should be associated with an acceptable toxicological profile. This design principle would deliver a prodrug to circulation that would be dependent upon enzyme-mediated cleavage to liberate **4**, which was anticipated to rearrange to **1** at physiological pH based on the *in vitro* analysis.

As the initial step in this direction, the conjugation of **4** with a non-basic but polar dioxolenone promoiety was explored, incorporated via a carbamate linker. This promoiety has found clinical application in the angiotensin II receptor antagonists, olmesartan medoxomil[30] and azilsartan medoxomil,[31] and the antibacterial agents, prulifloxacin[32] and ceftobiprole medocaril.[33] The dioxolenone prodrug **9** was derived in a single step upon treatment of **4** with the activated carbonate of 4-(hydroxymethyl)-5-methyl-1,3-dioxol-2-one (**8**),[34] as depicted in Scheme 4. This prodrug moiety was expected to undergo bioconversion in intestinal mucosa, the liver, and plasma by the action of multiple enzymes (especially carboxymethylenebutenolidase homologue and paraoxonase 1) to release the active parent **1** via **4** in addition to the byproducts carbon dioxide and diacetyl.[35−37] Prodrug **9** showed acceptable stability across a range of pH values, with an 18-fold

DOI: 10.1021/acs.jmedchem.8b00277
J. Med. Chem. XXXX, XXX, XXX−XXX

Table 2. Pharmacokinetic Data Obtained after Oral Administration of 1 at 3 mg/kg and Prodrugs at an Equivalent Dose of 3 mg/kg of Parent in SD Rats[a]

compound dosed	analyte	C_{max} (nM)	T_{max} (h)	AUC_{last} (nM·h)	%F	C_{trough} at 24 h (nM)	prodrug/parent ratio
1	**1**	266	0.5	384	20	0.25	NA
3	**1**	10	1.7	42	2.2	BLQ	112
	3	1529	0.5	4731	NA	1.09	
4	**1**	8	0.4	16	0.83[b]	BLQ	4.9
	4	68	0.3	79	NA	BLQ	
9	**1**	180	1.3	194	10.1[b]	0.3	0.1
	9	42	0.3	19	NA	BLQ	
11	**1**	56	0.4	83	4.3[b]	BLQ	NA
	11	4	0.3	1	NA	BLQ	
14	**1**	310	1.7	1446	75.3[b]	4.5	3.4
	4	124	1.7	579	NA	2.0	
	14	2160	0.4	4306	NA	10.0	
16	**1**	37	2.3	167	8.7[b]	0.3	50.5
	16	2209	0.3	8434	NA	49.7	

[a]Values shown are mean ± SD (n = 3). NA = not available, BLQ = below limit of quantification. The formulation used for these experiments was 10% v/v DMAc, 40% v/v PEG-400, 50% v/v of 30% w/v HPβCD in pH 4.0 citrate buffer (50 mM). [b]Relative F (oral bioavailability relative to that of **1**).

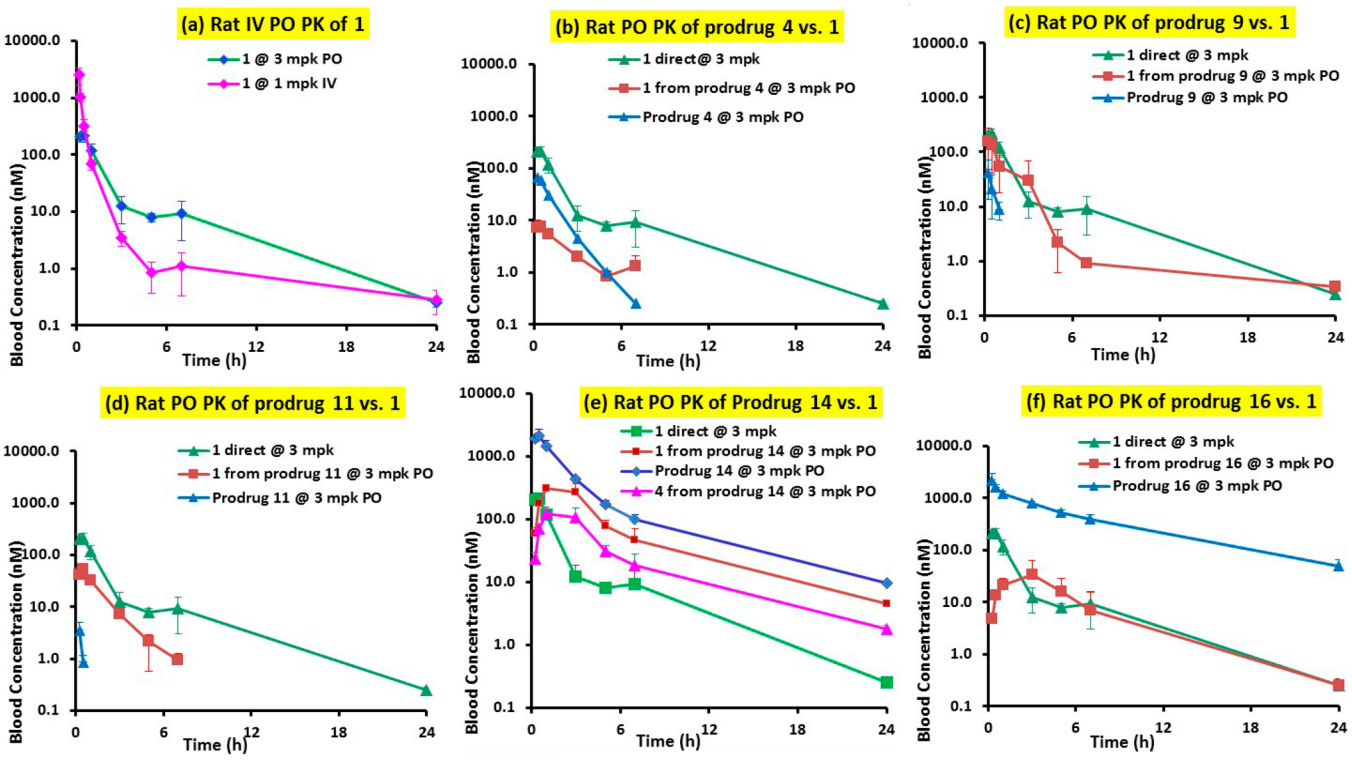

Figure 2. Exposure–time profiles obtained following oral administration of **1** and the prodrugs in SD rats.

improvement in solution stability at pH 6.5 when compared to **4**. Compound **9** exhibited pH-dependent solubility which was optimal only at acidic pH. Administration of **9** to rats resulted in the 12-fold improved exposure of **1** when compared to administration of **4**, but this was still lower than that of the directly dosed parent (Table 2 and Figure 2c). Plasma concentrations of intermediate **4** were not monitored in this study. Encouragingly, dosing of **9** resulted in a measurable C_{trough} concentration of **1** of 0.3 nM at 24 h post-dose, a contrast to the results observed with prodrug **4**. While this improvement was modest, it provided some confidence that improved intestinal stability would positively impact exposure. Inspired by this result, we examined optimization of the promoiety in an effort to further improve oral bioavailability.

The conjugation of **4** with amino acid esters was investigated next. Across therapeutic areas and drug classes, amino acid-based prodrugs have been reported to improve both solubility and absorption, some by relying on active transport, and to mitigate metabolic clearance of parent compounds.[39] The introduction of the amino acid side chain was accomplished through a carbamate-based methylene linker. Accordingly, **4** was treated with chloromethyl chloroformate to afford the less-stable chloromethyl carbamate derivative, which was subjected to *O*-alkylation with *N*-Boc-L-Val to afford the carbamate methylene *N*-Boc-L-Val derivative **10**. Deprotection of **10** by

DOI: 10.1021/acs.jmedchem.8b00277
J. Med. Chem. XXXX, XXX, XXX−XXX

Scheme 4. Carbamate-Based Conjugation of 4[a]

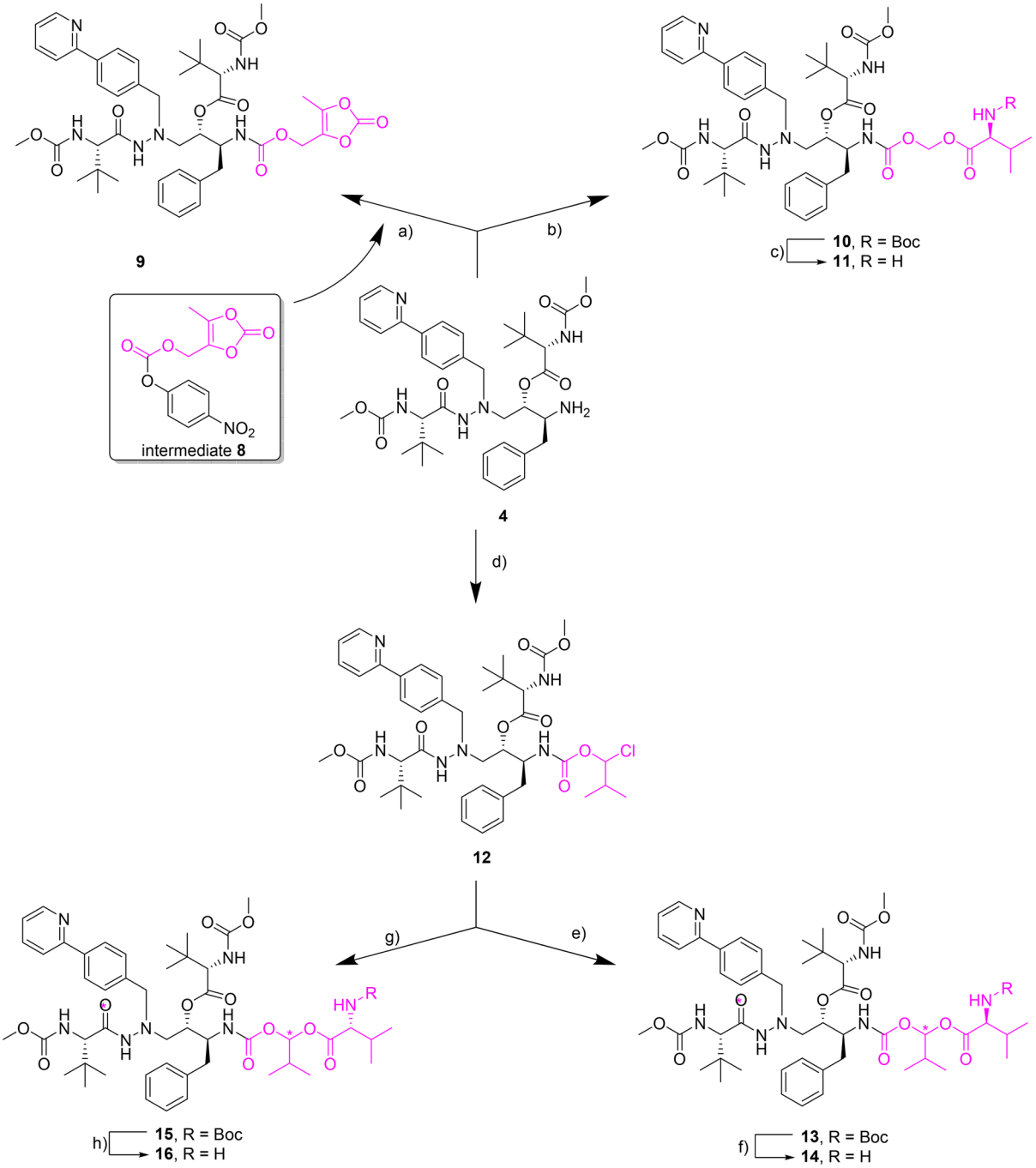

[a]Reagents and conditions: (a) (5-methyl-2-oxo-1,3-dioxol-4-yl)methyl (4-nitrophenyl) carbonate (**8**), DIPEA, DMAP, dioxane, 100 °C, 24 h, 10.1%; (b) (i) chloromethyl chloroformate, pyridine, DCM, 0 °C, 3 h, (ii) *N*-Boc-L-Val, NaI, DIPEA, DMF, 50 °C, 14 h, 26.5% for two steps; (c) 4 N HCl in dioxane, 0 °C, 1 h, 76%; (d) 2-chloro-2-methylpropyl chloroformate,[38] pyridine, DCM, 0 °C, 3 h, ~90%; (e) *N*-Boc-L-Val, NaI, DIPEA, DMF, 50 °C, 14 h, 29.7%; (f) 4 N HCl in dioxane, 0 °C, 1 h, 32%; (g) *N*-Boc-D-Val, NaI, DIPEA, DMF, 60 °C, 8 h, 31.9%; (h) 4 N HCl in dioxane, 0 °C, 1 h, 71.5%.

exposure to 4 N HCl in dioxane afforded the corresponding L-Val amino acid prodrug **11**. Assuming initial enzymatic cleavage of L-Val amino acid ester of this prodrug and subsequent spontaneous decomposition of the resultant intermediate **4** to release the parent, the prodrug can be expected to release L-Val, formaldehyde, and carbon dioxide as potential byproducts *in vivo* in the initial enzymatic step. Natural amino acids like L-Val, which serve as the building blocks of proteins, are ubiquitous in the human body, and hence the release of L-Val as a promoiety should not pose a significant safety concern.[39] L-Val was primarily selected as a prodrug moiety because of the clinical precedent of Val-based ester prodrugs in, for example, valacyclovir and valgancyclovir.[40] The potential for toxicity associated with the release of formaldehyde from a prodrug has been reviewed in context of the estimated daily exposure to this molecule in humans, where it is generated from a variety of endogenous and exogenous substrates.[41] Prodrug **11** displayed acceptable stability at pH 1 and 4 but significantly reduced

DOI: 10.1021/acs.jmedchem.8b00277
J. Med. Chem. XXXX, XXX, XXX−XXX

stability at the higher pH values relevant for absorption. At lower pH values, the amino acid ester prodrugs exist in the salt form, which confers good solubility. However, with increasing pH, the amine salt converts into the free amine, which may negatively impact solubility. Prodrug **11** showed excellent solubility at the tested pH range (pH 1−4) and exhibited 5-fold higher plasma exposure of **1** in rats compared to that delivered by **4** following oral administration (Table 2 and Figure 2d). However, this value was still lower than that obtained by dosing **1** directly. The trough concentration of **1**, which was released from **11**, was also BLQ. Intermediate **4** was not monitored for its systemic circulation in this study.

The poor stability of **11** at higher pH values prompted an investigation of the effect of installing alkyl substitution on the methylene bridge, assuming that such steric encumbrance around the carbamate and ester functionalities of the promoiety would reduce the hydrolytic lability.[42] The enhanced stability was expected to minimize the intestinal degradation of the prodrug and facilitate greater absorption of the prodrug itself. Accordingly, the carbamate-based isobutyl L-Val prodrug **14** was synthesized from **4** in three steps. Compound **4** was treated with 1-chloro-2-methylpropyl chloroformate[38] to afford crude product **12** which, due to modest stability, was immediately subjected to *O*-alkylation with *N*-Boc-L-Val to afford the carbamate isobutylene *N*-Boc-L-Val derivative **13**. Deprotection of **13** using 4 N HCl in dioxane afforded the corresponding L-Val amino acid prodrug **14**. Chiral HPLC analysis of **13** indicated the stereoisomeric purity of at least 95%, suggesting the possibility of a stereoselective *O*-alkylation.[43] The introduction of the isopropyl substituent resulted in an 16-fold increase in the chemical stability of **14** at pH 6.5 compared to the unsubstituted L-Val prodrug **11** (Table 1). Oral administration of **14** to SD rats resulted in a significant increase in the plasma levels of **1**, delivering a 90-fold higher exposure of **1** than prodrug **4** and a ∼4-fold higher exposure and 18-fold higher C_{trough} concentration of **1** than those following direct dosing of the parent drug (Table 2 and Figure 2e). Combining the exposure of circulating **14**, **4**, and **1**, the total exposure was 16-fold higher than that from the direct dosing of **1**. These results suggested that the prodrug not only was efficiently absorbed, but also was subject to reduced metabolic degradation by CYP enzymes.

Based on our design hypothesis, prodrug **14** is expected to undergo enzymatic hydrolysis as the first step to release intermediate **4** and equimolar amounts of L-Val, isobutyraldehyde, and carbon dioxide (Scheme 5). The intermediate **4** subsequently undergoes acyl migration-based degradation to release the parent. As a naturally occurring substance, isobutyraldehyde is encountered in several food items and metabolized to isobutyric acid, an intermediate in L-Val metabolism.[44] In addition, isobutyraldehyde is a food additive permitted for human consumption as a synthetic flavoring substance and adjuvant by the Federal Drug Administration (FDA). Clinical precedent for the release of isobutyraldehyde as a byproduct of prodrug activation is illustrated by the marketed drug fosinopril,[45] a prodrug of the phosphinic acid-based angiotensin-converting enzyme inhibitor fosinoprilat, and arbaclofen placarbil,[46] a prodrug of the gamma amino butyric acid type B receptor agonist arbaclofen.

The parallel PK profiles of **14** and **4** depicted in Figure 2e suggest that **14** acts as a depot, steadily releasing **4** which then converts into **1** in the systemic circulation, reflecting a formation rate-mediated clearance of **1**. The observation of **4** in plasma supports a stepwise activation process involving cleavage of conjugate **14** to release **4**, which then undergoes acyl migration to afford **1**. The lower AUC of **4** compared to **1** and **14** reflects the different rates of activation of **4** and **14**, with the enzyme-mediated cleavage as the rate-determining step. Interestingly, the plasma exposure profiles of **4** and **1** differ depending on whether **4** or **14** is dosed (Table 2). Dosing of **4** provides a 5-fold higher plasma exposure of this prodrug than for **1**. However, after dosing **14**, the ratio of **4** to **1** is inverted and 2.5-fold in favor of the parent drug. Because the generation of **1** from **14** without the intervention of **4** is limited, a potential explanation may include a nonlinear increase in **1** from the higher concentration of **4** in plasma or a more rapid rate of conversion of **4** to **1** when **4** is enzymatically released from **14**.

Because prodrugs **4** and **14** mask the transition-state-mimicking, pharmacophoric secondary alcohol moiety of **1**, they would not be expected to be effective HIV-1 PIs. However, prodrug **14** demonstrated antiviral activity in an HIV-1 infection assay (EC_{50} = 5.3 nM), suggesting that in cell culture the prodrug can undergo bioactivation and conversion to generate **1**, which mediates the antiviral activity. Similarly, the intermediate prodrug **4** showed high functional potency (EC_{50}

Scheme 5. Potential *in Vivo* Degradation Pathway of the Conjugative Acyl Migration Prodrug 14 To Release the Parent Drug 1

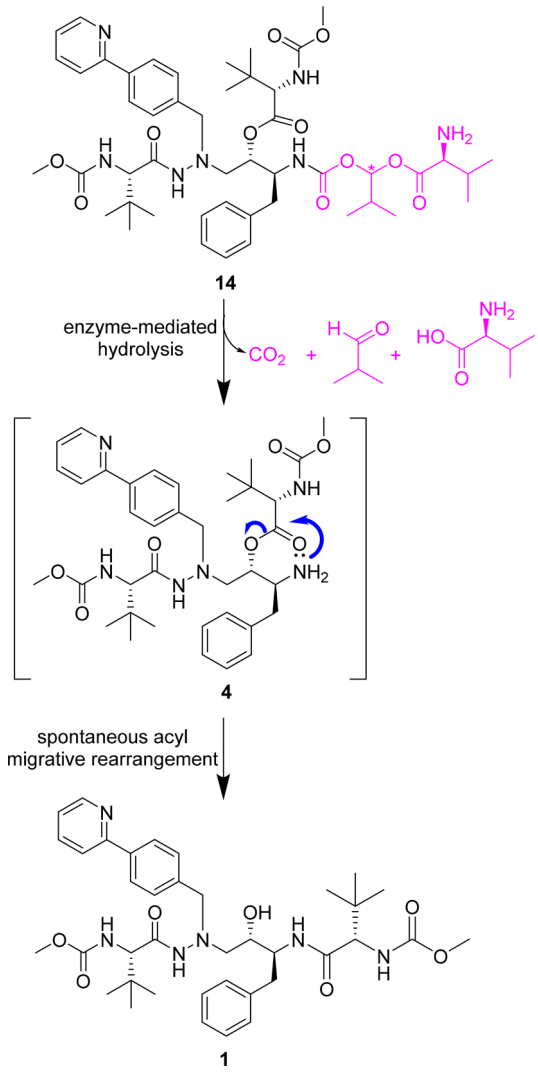

DOI: 10.1021/acs.jmedchem.8b00277
J. Med. Chem. XXXX, XXX, XXX−XXX

= 1.8 nM). However, both sets of data reflect some limitation on parent drug release in this setting since the EC_{50} value for **1** was 0.7 nM.

Prodrug **16**, a diastereomer of **14**, was synthesized next by replacing L-Val with D-Val in order to understand the impact of absolute configuration on stability, solubility, and the PK profile. Accordingly, **16** was synthesized by treating the 1-chloro-2-methylpropyl carbamate derivative **12** with *N*-Boc-D-Val to afford the carbamate isobutylene *N*-Boc-D-Val ester **15** and subsequent deprotection of **15** using HCl. Analogous to the observation for **13**, chiral HPLC analysis of **15** indicated a chiral purity of at least 95%, suggestive of a stereoselective reaction. The D-Val prodrug **16** showed higher stability at pH 6.5 and higher solubility at pH 4 and 6.5 than the L-Val prodrug **14**. In SD rats, oral dosing of **16** produced a 9-fold lower exposure of **1** than **14** but a 2-fold higher exposure of the circulating prodrug than **14** (Table 2 and Figure 2f). The prodrug-to-parent ratio observed in the case of **16** was 15-fold higher when compared to that of **14**. This is consistent with a lower rate of activation of the D-Val prodrug **16** than the L-Val-based **14**. This can be rationalized by slower cleavage of the unnatural D-Val amino acid by hydrolytic enzymes compared to the prodrug based on natural L-Val. Combining the exposure of **16** and **1**, the total AUC was 22-fold higher than that from direct dosing of **1**, suggesting more efficient absorption and lower metabolic clearance of this prodrug than the parent. As in the case of **14**, the *in vivo* cleavage of **16** to generate **1** presumably results from an initial enzymatic step that involves the release of acyl migration intermediate **4** and equimolar amounts of D-Val, isobutyraldehyde, and carbon dioxide.

This double prodrug approach was essential because the simple L-Val ester **3**, which may be preferred for practical reasons associated with ease of synthesis, performed poorly following oral administration to rats. Dosing of **3** gave 9-fold lower exposure of **1** than direct administration of the drug itself and 34-fold lower exposure than the exposure of the parent **1** released following administration of the acyl migration L-Val prodrug **14** (Figure 4).

The improved combined exposure of **1** and the prodrug following oral dosing of **14** and **16** (Figure 3) can be attributed to several factors, including improved aqueous solubility (Table 1), reduced efflux, and reduced susceptibility to CYP 450-mediated metabolism (Table 3). Although these conjugates do not exhibit higher absorptive permeability in heterogeneous human epithelial colorectal adenocarcinoma (Caco-2) cells than the parent or acyl migration prodrug **4**, they have shown significantly lower efflux which could, in part, contribute to the improved exposure. These results suggest that conjugation of **4** as carbamate isobutylene Val derivatives contributed to reduced affinity for efflux transporters. Prodrugs **14** and **16** were incubated in rat hepatocytes, considered to be better predictors of metabolism *in vivo* than liver microsomal preparations because they express all hepatic metabolizing enzymes.[47] Both **14** and **16** exhibited improved half-lives compared to **1**, suggesting that the prodrugs were less prone to metabolic degradation than the parent drug. The rat whole blood stability profile of **14** and **16** indicates high stability, which is consistent with the observed slow rate of cleavage *in vivo*, which is presumably mediated by esterases or peptidases, leading to a circulating depot of **14** and **16** that slowly releases **1** *in vivo*.

With the promising PK data in hand, the effect of gastric pH on delivery of **1** by **14** was examined using a suspension formulation evaluated in a rat model where gastric pH was modulated by treatment with either pentagastrin or famotidine.[9,10,48] **1** is known to depend upon an acidic gastric environment for adequate dissolution and subsequent absorption *in vivo*.[9,10] Concomitant administration of PPIs and **1** is currently not recommended because as acid-suppressing agents, PPIs are known to reduce the exposure of **1**, thereby increasing the risk of sub-optimal therapy and resistance development.[49] Following oral administration of **14** to male SD rats, there was no significant difference in the systemic exposure of **1** and **14** by pre-treatment with either pentagastrin to enhance stomach acidity or famotidine to reduce acidity, as depicted in Figure 5. In contrast, a 492-fold

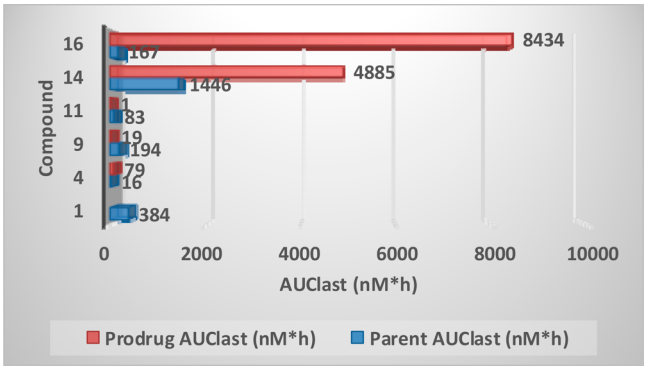

Figure 3. Comparative chart of exposures of prodrug and parent, indicating the superior performance of prodrugs **14** and **16** when compared to unconjugated acyl migration prodrug **4** or its other conjugates. For prodrug **14**, the combined AUC of **14** and its intermediate **4** [4306 + 579 nM·h] is included.

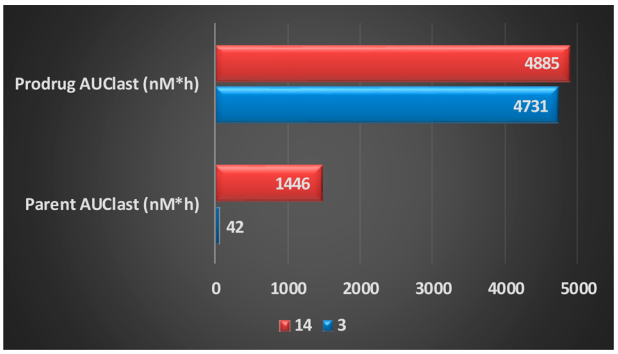

Figure 4. Comparative chart, indicating superior oral delivery of **1** from acyl migration L-Val prodrug **14** compared to simple direct L-Val ester **3**. For prodrug **14**, the combined AUC of **14** and its intermediate **4** [4306 + 579 nM·h] is included.

Table 3. Bidirectional Caco-2 Permeability and *in Vitro* Metabolic Stability Data

	P_{app} (nm/s)			$t_{1/2}$ (min)	
parent/ prodrug	Caco-2 A-B[a]	Caco-2 B-A[b]	Caco-2 efflux ratio	rat hepatocytes	rat whole blood
1	<15	470	>31	28	>120
4	23	348	15	79	>120
9	ND	ND	ND	<5	<5
11	ND	ND	ND	<5	20
14	<15	114	>8	56	>120
16	<15	73	>5	53	>120

[a]Apical-to-basolateral direction. [b]Basolateral-to-apical direction.

DOI: 10.1021/acs.jmedchem.8b00277
J. Med. Chem. XXXX, XXX, XXX−XXX

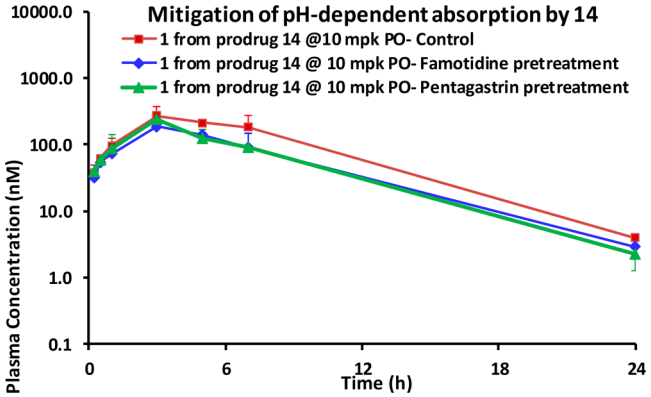

Figure 5. AUC profiles of **1**, obtained following oral administration of the prodrug **14** in a rat pH model study using a suspension formulation of 0.5% methyl cellulose and 99.5% water.

difference in systemic exposure was observed between the pentagastrin and famotidine arms following direct administration of **1** (Figure 6).[48] These data suggest that **14** is able to

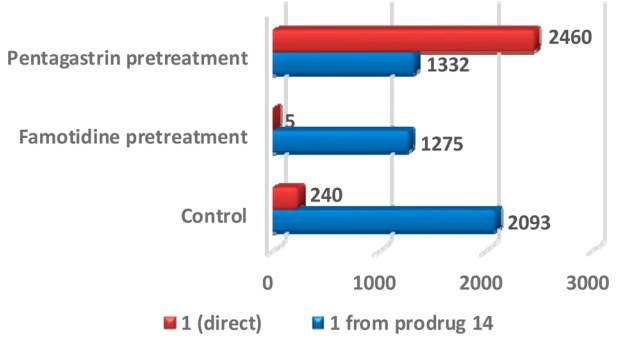

Figure 6. Comparison of $AUC_{0-24\ h}$ profiles of **1**, obtained following oral administration of **14** and **1** itself in the rat pH model. Data for the direct dosing of **1** taken from ref 48.

substantially mitigate pH-dependent absorption in rats and hence may offer the benefit of reduced drug−drug interaction with PPIs, thereby potentially improving the profile of the agent. The lack of the pH effect on absorption of **14** may be attributed to higher solubility and/or a salt form that can drive dissolution and kinetic solubility.

CONCLUSIONS

In conclusion, the reported results suggest that a conjugative acyl migration prodrug design principle can be useful as a drug delivery approach to significantly improve the oral bioavailability of **1**, with the advantage that a circulating prodrug results in an extended release of parent drug that is reflected in a higher C_{trough} concentration. Such a novel drug delivery is warranted in the light of the drug delivery challenges, reported with the direct ester prodrugs of PIs, including the direct L-Val ester of **1**. This conjugation, engineered to undergo a sequential bio- and chemo-activation process, was found to play a critical role in the enhanced exposure of **1**, since the simple acyl migration prodrug **4** failed to deliver a significant amount of the parent *in vivo*. Additionally, the lead prodrug **14** demonstrated potential to mitigate the drug−drug interaction observed between the parent drug and PPIs, as evident from the pH effect study. The prodrug demonstrated potent antiviral activity, which suggested efficient cellular penetration and conversion to **1** that was responsible for the activity. The reduced metabolism of **14** and **16**, as determined from *in vitro* studies, and the improved exposure suggest that the prodrugs mitigate, in part, the major limitation of CYP3A metabolism. This discovery opens opportunities for the development of metabolism-mitigating, depot-acting prodrugs. However, this approach will require (1) refinement of prodrug cleavage *in vivo*, especially, for achieving dose-proportional exposure, (2) understanding the performance of the prodrug *in vivo* in higher species and the potential for cross-species differences in enzymatic cleavage of the prodrug moiety, and (3) assessment of the potential safety and other liabilities [for example, profiling for hERG and CYP2D6 inhibition due to the presence of an ionizable amine in the promoiety and for hepatic uridine diphosphate glucuronosyltransferase 1A1 (UGT1A1) inhibition to assess hyperbilirubinemia potential because of the known inhibition of UGT1A1 by the parent drug] associated with developing a prodrug with high and sustained oral exposure.

EXPERIMENTAL SECTION

Materials and General Methods. All anhydrous reactions were performed under an atmosphere of N_2 or Ar gas with magnetic stirring. All reagents and solvents were purchased from commercial suppliers (e.g., Aldrich, Alfa, Acros, Spectrochem, and Sonia) and were used without further purification, unless otherwise stated. Reactions were monitored by thin layer chromatography (TLC) or LC/MS. TLC was performed using E. Merck pre-coated silica plates (60F-254) with 0.25 mm thickness and visualized using short-wave UV light or developing agents ($KMnO_4$, phosphomolybdic acid, or *p*-anisaldehyde). For LC/MS monitoring, samples were run on a Waters Aquity system coupled with a Waters Micromass SQ Mass Spectrometer (buffer, 10 mM ammonium acetate or 0.01% trifluoroacetic acid; run time, 3 min; flow rate, 0.7 mL/min). Crude compounds were purified by either normal phase column chromatography using a Teledyne ISCO CombiFlash system or reverse phase chromatography using preparative HPLC instruments (Agilent 1200 series) equipped with a high-pressure quaternary pump, a diode array detector, and a universal loop injector with different C18 columns, for example, Sunfire, XBridge phenyl, and Kinetex.

Analytical purity of the compounds was determined by HPLC analysis to be ≥95%, unless otherwise noted. The following HPLC methods were used to determine the analytical purity of the compounds.

(i) Analytical HPLC method A: column = Sunfire C18 [150 × 4.6 mm] 3.5 μm; buffer = 0.05% trifluoroacetic acid in water; mobile phase A = buffer:MeCN [95:5]; mobile phase B = MeCN:buffer [95:5]; 10% B to 100% B; run time = 23 min; flow rate = 1.0 mL/min).

(ii) Analytical HPLC method B: column = XBridge phenyl C18 [150 × 4.6 mm] 3.5 μm; buffer = 0.05% trifluoroacetic acid in water; mobile phase A = buffer: MeCN [95:5]; mobile phase B = MeCN: buffer [95:5]; 10% B to 100% B; run time = 23 min; flow rate = 1.0 mL/min).

(iii) Analytical HPLC method C: column = Kinetex Evo C18 [100 × 4.6 mm] 2.6 μm; buffer = 0.05% trifluoroacetic acid in water; mobile phase A = buffer: MeCN [95:5]; mobile phase B = MeCN: buffer [95:5]; 10% B to 100% B; run time = 23 min; flow rate = 1.0 mL/min).

(iv) Analytical HPLC method D: column = Kinetex Biphenyl C18 [100 × 4.6 mm] 2.6 μm; buffer = 0.05% trifluoroacetic acid in water; mobile phase A = buffer: MeCN [95:5]; mobile phase B = MeCN: buffer [95:5]; 10% B to 100% B; run time = 23 min; flow rate = 1.0 mL/min).

Chiral purity was determined by the following methods on a Agilent HPLC SFC hybrid instrument using CHIRALPAK columns:

DOI: 10.1021/acs.jmedchem.8b00277
J. Med. Chem. XXXX, XXX, XXX−XXX

(i) Chiral HPLC method A: column = CHIRALPAK IC [250 × 4.6 mm] 5.0 μm; co-solvent: 0.2% ammonia in CH_3CN:MeOH (1:1 mixture); run time = 15 min; flow rate = 4 mL/min).
(ii) Chiral HPLC method B: column = CHIRALPAK ID [250 × 4.6 mm] 5.0 μm; co-solvent: 0.2% ammonia in CH_3CN:MeOH (1:1 mixture); run time = 15 min; flow rate = 4 mL/min).

Known compounds were characterized by comparing their ^{1}H NMR spectra to the previously reported data. New compounds were characterized by ^{1}H NMR and MS. Proton nuclear magnetic resonance (^{1}H NMR) spectra were recorded on Bruker 300 and 400 MHz instruments. Chemical shifts are reported in ppm (δ) relative to the internal standard tetramethylsilane (TMS, δ 0.00 ppm). NMR data are reported as follows: chemical shift (multiplicity [singlet (s), doublet (d), triplet (t), quartet (q), pentet (p), multiplet (m), and broad singlet (br s)], coupling constant [Hz], and integration). For LC/MS characterization of the compounds, reverse phase analytical HPLC/MS experiments were performed on Agilent 1200 Series system coupled with a single quadrupole instrument (ESI) or Waters Aquity system coupled with a Waters Micromass SQ Mass Spectrometer. HRMS data were obtained on an Agilent HPLC/Q-TOF G6540A mass spectrometer using APPI or APCI methods in positive or negative ion detection modes.

Experimental Procedures. *(2S,3S)-3-((S)-2-((Methoxycarbonyl)-amino)-3,3-dimethylbutanamido)-1-(2-((S)-2-((methoxycarbonyl)-amino)-3,3-dimethylbutanoyl)-1-(4-(pyridin-2-yl)benzyl)-hydrazinyl)-4-phenylbutan-2-yl (tert-Butoxycarbonyl)-L-valinate (**2**).* To a solution of atazanavir (0.200 g, 0.284 mmol) in anhydrous DCM (5.0 mL) were sequentially added (*tert*-butoxycarbonyl)-L-valine (0.92 g, 0.426 mmol), DCC (0.117 g, 0.567 mmol), and DMAP (34.8 mg, 0.284 mmol). The reaction mixture was stirred at room temperature for 12 h and filtered through a Celite bed. The Celite bed was washed with ethyl acetate. The filtrate was concentrated *in vacuo*. The resulting crude compound was purified by preparative HPLC (preparative HPLC conditions: column: XBridge phenyl C18 (19 × 250 mm; 5 μm); mobile phase A: 10 mM ammonium acetate in water; mobile phase B: acetonitrile; flow rate: 20 mL/min; gradient: 0/50, 11/80). The pooled HPLC fraction was concentrated under reduced pressure at 30 °C. The residue was then dissolved in a solvent mixture of acetonitrile and water, and the solution was lyophilized for 12 h to obtain the title product as an off-white solid (190 mg, 74.1%). ^{1}H NMR (400 MHz, DMSO-d_6) δ = 8.86 (br s, 1H), 8.65 (d, J = 4.5 Hz, 1H), 7.97−7.82 (m, 4H), 7.79−7.68 (m, 1H), 7.42−7.28 (m, 4H), 7.20−7.10 (m, 5H), 6.80−6.59 (m, 2H), 4.94 (br s, 1H), 4.72−4.51 (m, 1H), 4.02−3.84 (m, 4H), 3.66 (d, J = 9.1 Hz, 1H), 3.55 (s, 3H), 3.41 (s, 3H), 3.00 (br s, 2H), 2.64 (d, J = 7.2 Hz, 2H), 2.19−2.02 (m, 1H), 1.38 (s, 9H), 0.94 (d, J = 6.8 Hz, 6H), 0.84 (s, 9H), 0.74 (s, 9H); MS (ES): m/z 905.4 [M+H]$^+$. Analytical HPLC-RT and purity: method C = 4.168 min and 99.95%; method D = 5.973 min and 99.94%. HRMS (ESI/Orbitrap) m/z: [M+H]$^+$ calcd for $C_{48}H_{70}N_7O_{10}$ 904.5179; found 904.5161.

*(2S,3S)-3-((S)-2-((Methoxycarbonyl)amino)-3,3-dimethylbutan-amido)-1-(2-((S)-2-((methoxycarbonyl)amino)-3,3-dimethyl-butanoyl)-1-(4-(pyridin-2-yl)benzyl)hydrazinyl)-4-phenylbutan-2-yl L-Valinate Dihydrochloride (**3**).* In a 5 mL round-bottom flask, (2*S*,3*S*)-3-((*S*)-2-((methoxycarbonyl)amino)-3,3-dimethylbutan-amido)-1-(2-((*S*)-2-((methoxycarbonyl)amino)-3,3-dimethyl-butanoyl)-1-(4-(pyridin-2-yl)benzyl)hydrazinyl)-4-phenylbutan-2-yl (*tert*-butoxycarbonyl)-L-valinate (**2**) (0.065 g, 0.072 mmol) was taken and cooled to 0 °C. A solution of 4 M HCl in diethyl ether (1.80 mL, 7.19 mmol) was added, and the reaction mixture was stirred at 0 °C for 1 h. The mixture was then concentrated under vacuum. The residue was dissolved in a mixture of acetonitrile and water. The resultant mixture was frozen and lyophilized for 12 h to get the title product as an off-white solid (55 mg; 85%). ^{1}H NMR (300 MHz, D_2O) δ 8.71−8.65 (m, 1H), 8.60−8.51 (m, 1H), 8.25−8.18 (m, 1H), 7.97−7.88 (m, 1H), 7.83−7.72 (m, 2H), 7.64−7.57 (m, 2H), 7.29−7.11 (m, 5H),5.22−5.10 (m, 1H), 4.11−3.71 (m, 5H), 3.63−3.36 (m, 7H), 3.04−2.87 (m, 3H), 2.68−2.39 (m, 2H), 1.13−0.96 (m, 6H), 0.71 (s, 9H), 0.67 (s, 9H); (ES): m/z 804.9 [M+H]$^+$. Analytical HPLC-RT and purity: method A = 6.17 min and 97.8%; method B = 6.96 min and 98.6%. HRMS (ESI/Orbitrap) m/z: [M+H]$^+$ calcd for $C_{43}H_{62}N_7O_8$ 804.4654; found 804.4649.

*(2S,3S)-3-Amino-1-(2-((S)-2-((methoxycarbonyl)amino)-3,3-dimethylbutanoyl)-1-(4-(pyridin-2-yl)benzyl)hydrazinyl)-4-phenyl-butan-2-yl (S)-2-((Methoxycarbonyl)amino)-3,3-dimethylbutanoate Dihydrochloride (**4**).* To the solid of (5*S*,10*S*,11*S*)-11-benzyl-5-(*tert*-butyl)-15,15-dimethyl-3,6,13-trioxo-8-(4-(pyridin-2-yl)benzyl)-2,14-dioxa-4,7,8,12-tetraazahexadecan-10-yl (*S*)-2-((methoxycarbonyl)-amino)-3,3-dimethylbutanoate (**7**) (800 mg, 0.994 mmol) was added 4 N HCl in dioxane (4.75 mL, 19.88 mmol) at 0 °C under nitrogen atmosphere. After being stirred at 0 °C for 1 h, the reaction mixture was concentrated *in vacuo* at 30 °C. The residue was stirred with ether. The solvent was carefully decanted. The resultant solid was dried under vacuum to get crude product as an off-white solid. The solid was dissolved in a solvent mixture of acetonitrile and water. The resulting mixture was frozen and lyophilized for 12.0 h to afford the title product (700 mg; 87%) as a colorless solid. ^{1}H NMR (400 MHz, DMSO-d_6) δ 9.65−9.45 (m, 1H), 8.78−8.69 (m, 1H), 8.67−8.55 (m, 2H), 8.16−8.03 (m, 2H), 7.98 (d, J = 8.0 Hz, 2H), 7.74−7.63 (m, 1H), 7.57−7.49 (m, 1H), 7.43 (d, J = 8.5 Hz, 2H), 7.32 (d, J = 7.5 Hz, 3H), 7.20 (s, 2H), 7.02−6.80 (m, 1H), 5.06−4.88 (m, 1H), 4.14−3.86 (m, 4H), 3.70−3.65 (m, 3H), 3.41 (s, 4H), 3.24−3.08 (m, 2H), 3.05−2.93 (m, 1H), 2.91−2.77 (m, 1H), 0.98 (s, 9H), 0.62 (s, 9H); MS (ES): m/z 705.4 [M+H]$^+$. Analytical HPLC purity and retention time: method A = 95.61% and 6.498 min; method B = 98.81% and 7.913 min. HRMS (ESI/Orbitrap) m/z: [M+H]$^+$ calcd for $C_{38}H_{53}N_6O_7$ 705.3970; found 705.3966.

*(S)-2-((Methoxycarbonyl)amino)-3,3-dimethylbutanoic Acid (**6**).*[29] To a stirred solution of (*S*)-2-amino-3,3-dimethylbutanoic acid (10.0 g, 76 mmol) in anhydrous 1,4-dioxane (50 mL) were sequentially added a solution of 2 M sodium hydroxide (114 mL, 229 mmol) and methyl chloroformate (11.78 mL, 152 mmol) at 0 °C dropwise. The reaction mixture was stirred at 60 °C for 18 h. The mixture was subsequently cooled to ambient temperature and extracted with DCM. The aqueous layer was acidified with 1.5 N HCl. The resulting solution was extracted with ethyl acetate. The organic layer was washed with brine solution, dried over anhydrous sodium sulfate, filtered, and concentrated under vacuum to get the crude product as a colorless oil, which was stirred in hexane. The precipitated solid was filtered and dried to get the title product (12.0 g, 63.4 mmol, 83%) as a colorless solid. ^{1}H NMR (300 MHz, DMSO-d_6) δ 12.48 (br s, 1H), 7.26 (d, J = 9.1 Hz, 1H), 3.79 (d, J = 9.1 Hz, 1H), 3.54 (s, 3H), 0.94 (s, 9H).

*(5S,10S,11S)-11-Benzyl-5-(tert-butyl)-15,15-dimethyl-3,6,13-trioxo-8-(4-(pyridin-2-yl)benzyl)-2,14-dioxa-4,7,8,12-tetraazahexa-decan-10-yl (S)-2-((Methoxycarbonyl)amino)-3,3-dimethylbuta-noate (**7**).* To a solution of methyl ((*S*)-1-(2-((2*S*,3*S*)-3-((*tert*-butoxycarbonyl)amino)-2-hydroxy-4-phenylbutyl)-2-(4-(pyridin-2-yl)-benzyl)hydrazinyl)-3,3-dimethyl-1-oxobutan-2-yl)carbamate (**5**) (3 g, 4.73 mmol) in DCM (20 mL) were added (*S*)-2-((methoxycarbonyl)-amino)-3,3-dimethylbutanoic acid **6** (1.343 g, 7.10 mmol), dicyclo-hexylcarbodiimide (1.953 g, 9.47 mmol), and 4-dimethylamino-pyridine (0.578 g, 4.73 mmol). The reaction mixture was stirred at room temperature for 12 h and filtered through a Celite bed, which was subsequently washed with ethyl acetate. The combined filtrate was concentrated *in vacuo* at 30 °C. The crude product was purified by RP HPLC (preparative HPLC conditions: Sunfire C18 (250 × 30 mm; 5 μm), mobile phase A: 10 mM ammonium acetate in water at pH 4.5, mobile phase B: acetonitrile, flow rate: 27 mL/min, gradient: 0/50, 7/85). The pooled HPLC fraction was concentrated *in vacuo* at 30 °C. The residue was dissolved in a solvent mixture of acetonitrile and water. The resultant mixture was lyophilized for 12 h to get the title product as a white solid (2 g; 52.5%). ^{1}H NMR (400 MHz, MeOH-d_4) δ 8.65−8.56 (m, 1H), 7.94−7.78 (m, 4H), 7.48 (d, J = 8.0 Hz, 3H), 7.36 (ddd, J = 7.4, 4.9, 1.3 Hz, 1H), 7.30−7.14 (m, 5H), 6.63−6.46 (m, 1H), 5.21−5.05 (m, 1H), 4.38−4.26 (m, 1H), 4.22−4.01 (m, 3H), 3.78−3.65 (m, 4H), 3.54 (s, 3H), 3.30−3.22 (m, 1H), 3.15−3.03 (m, 1H), 2.80 (br s, 1H), 2.73−2.58 (m, 1H), 2.17 (s, 1H), 1.33 (s, 7H), 1.20 (s, 2H), 1.09 (s, 9H), 0.82 (s, 9H); MS (ES): m/z 805.4 [M+H]$^+$.

DOI: 10.1021/acs.jmedchem.8b00277
J. Med. Chem. XXXX, XXX, XXX−XXX

HRMS (ESI/Orbitrap) m/z: $[M+H]^+$ calcd for $C_{43}H_{61}N_6O_9$ 805.4495; found 805.4465.

*(5-Methyl-2-oxo-1,3-dioxol-4-yl)methyl (4-Nitrophenyl) Carbonate (**8**).*[34] A stirred solution of 4-(hydroxymethyl)-5-methyl-1,3-dioxol-2-one (1.4 g, 10.76 mmol) in DCM (15 mL) was cooled to 0 °C. Pyridine (8.70 mL, 108 mmol) was added, and the reaction mixture was stirred for 5 min. Then 4-nitrophenyl chloroformate (8.68 g, 43.0 mmol) was added, and the reaction mixture was stirred at room temperature for 24 h. Water was added. The reaction mixture was extracted with DCM (3 × 50 mL). The combined organic layer was washed with 1.5 N HCl and brine, dried over anhydrous sodium sulfate, filtered, and concentrated to get a brownish gum. The crude product was purified by CombiFlash (silica gel 60−120 mesh; 50% ethyl acetate in hexane as an eluent) to get the title product (1.8 g, 5.98 mmol, 55.5%) as a white solid. ^{1}H NMR (300 MHz, $CHCl_3$-*d*) δ 8.35−8.26 (m, 2H), 7.44−7.37 (m, 2H), 5.04 (s, 2H), 2.23 (s, 3H). MS (ES): The desired mass peak was not obtained.

*(5S,10S,11S)-11-Benzyl-5-(tert-butyl)-15-(5-methyl-2-oxo-1,3-dioxol-4-yl)-3,6,13-trioxo-8-(4-(pyridin-2-yl)benzyl)-2,14-dioxa-4,7,8,12-tetraazapentadecan-10-yl (S)-2-((Methoxycarbonyl)amino)-3,3-dimethylbutanoate (**9**).* To a stirred solution of (2*S*,3*S*)-3-amino-1-(2-((*S*)-2-((methoxycarbonyl)amino)-3,3-dimethylbutanoyl)-1-(4-(pyridin-2-yl)benzyl)hydrazinyl)-4-phenylbutan-2-yl (*S*)-2-((methoxycarbonyl)amino)-3,3-dimethylbutanoate dihydrochloride (**4**) (0.3 g, 0.386 mmol) in dioxane (10 mL) were added DIPEA (0.202 mL, 1.157 mmol), DMAP (0.024 g, 0.193 mmol), and (5-methyl-2-oxo-1,3-dioxol-4-yl)methyl (4-nitrophenyl) carbonate **8** (0.228 g, 0.771 mmol). The reaction mixture was heated at 100 °C for 24 h and cooled to ambient temperature. The reaction mixture was concentrated under reduced pressure to remove the solvent. The residue was partitioned between water and ethyl acetate. The organic layer was washed with brine, dried over anhydrous sodium sulfate, filtered, and concentrated to get a brownish gum. The crude product was purified using RP-HPLC (preparative HPLC conditions: Sunfire C18 (150 × 19 mm; 5 μm), mobile phase A: 10 mM ammonium acetate in water at 4.5 pH, mobile phase B: acetonitrile, flow rate: 17 mL/min, gradient: 0/30, 7/65). The fraction was concentrated using high vacuum at 30 °C. The residue was dissolved in a mixture of acetonitrile and water. The mixture was frozen and lyophilized for 12 h to get the title product (0.035 g, 0.039 mmol, 10.09% yield) as a white solid. ^{1}H NMR (400 MHz, MeOH-d_4) δ 8.61 (td, J = 2.5, 1.0 Hz, 1H), 7.94−7.82 (m, 4H), 7.51 (d, J = 8.0 Hz, 2H), 7.36 (ddd, J = 7.3, 5.0, 1.3 Hz, 1H), 7.30−7.12 (m, 5H), 5.12 (br s, 1H), 4.81 (d, J = 14.1 Hz, 1H), 4.62 (d, J = 14.1 Hz, 1H), 4.42 (br s, 1H), 4.18−4.00 (m, 3H), 3.74 (s, 1H), 3.70 (s, 3H), 3.54 (s, 3H), 3.28−3.19 (m, 1H), 3.18−3.04 (m, 1H), 2.84 (dd, J = 13.6, 5.0 Hz, 1H), 2.67−2.55 (m, 1H), 2.03 (s, 3H), 1.07 (s, 9H), 0.84 (s, 9H); LCMS (ES): m/z 861.4 $[M+H]^+$. Analytical HPLC RT and purity: method A = 7.85 min and 95.78%; method B = 9.32 min and 95.88%. HRMS (ESI/Orbitrap) m/z: $[M+H]^+$ calcd for $C_{44}H_{57}N_6O_{12}$ 861.4029; found 861.3986.

*(5S,10S,11S,18S)-11-Benzyl-5-(tert-butyl)-18-isopropyl-22,22-dimethyl-3,6,13,17,20-pentaoxo-8-(4-(pyridin-2-yl)benzyl)-2,14,16,21-tetraoxa-4,7,8,12,19-pentaazatricosan-10-yl (S)-2-((Methoxycarbonyl)amino)-3,3-dimethylbutanoate (**10**).* To a solution of (2*S*,3*S*)-3-amino-1-(2-((*S*)-2-((methoxycarbonyl)amino)-3,3-dimethylbutanoyl)-1-(4-(pyridin-2-yl)benzyl)hydrazinyl)-4-phenylbutan-2-yl (*S*)-2-((methoxycarbonyl)amino)-3,3-dimethylbutanoate dihydrochloride (**4**) (300 mg, 0.426 mmol) in DCM (2 mL) were added pyridine (0.172 mL, 2.128 mmol) and chloromethyl chloroformate (0.076 mL, 0.851 mmol) under nitrogen atmosphere. After being stirred at 0 °C for 3 h, the reaction mixture was partitioned between 1.5 N HCl and DCM. The organic layer was washed with water and brine, dried over anhydrous sodium sulfate, and concentrated under vacuum to get the crude product as an off-white solid (300 mg). MS (ES): m/z 797.4 $[M+H]^+$. To the solution of this crude product in DMF (1 mL) were added *N*-Boc-L-Val (123 mg, 0.564 mmol), DIPEA (0.329 mL, 1.881 mmol), and sodium iodide (56.4 mg, 0.376 mmol). The reaction mixture was heated at 50 °C for 14 h. The reaction mixture was partitioned between water and EtOAc. The organic layer was washed with water and brine, dried over anhydrous sodium sulfate, and concentrated under vacuum to get the crude product as a light brownish oil, which was purified by RP HPLC (preparative HPLC conditions: X Bridge phenyl 250 × 19 mm; mobile phase A: 10 mM ammonium acetate in water at pH 4.5; mobile phase B: acetonitrile; flow rate: 17 mL/min.; isocratic mobile phase A:B = 40:60 with a run time of 30 min). The HPLC fraction was concentrated under reduced pressure at ∼30 °C. The residue was dissolved in a solvent mixture of acetonitrile and water, and frozen solution was lyophilized for 12 h to get the title product as an off-white solid (100 mg; 26.5% for two steps).^{1}H NMR (400 MHz, MeOH-d_4) δ 8.66−8.55 (m, 1H), 7.93−7.80 (m, 4H), 7.51−7.48 (m, 2H), 7.40−7.34 (m, 1H), 7.30−7.15 (m, 5H), 5.73−5.60 (m, 2H), 5.12−5.03 (m, 1H), 4.56−4.47 (m, 1H), 4.20−4.09 (m, 2H), 4.06−3.95 (m, 2H), 3.70 (s, 4H), 3.53 (s, 3H), 3.28−3.19 (m, 1H), 3.12−3.02 (m, 1H), 2.91−2.78 (m, 1H), 2.76−2.66 (m, 1H), 2.10−1.99 (m, 1H), 1.43 (s, 9H), 1.07 (s, 9H), 0.93−0.84 (m, 6H), 0.80 (s, 9H); MS (ES): m/z 978.4 $[M+H]^+$. Analytical HPLC-RT and purity: method A = 10.349 min and 97.63%; method B = 10.861 min and 99.57%. HRMS (ESI/Orbitrap) m/z: $[M+H]^+$ calcd for $C_{50}H_{72}N_7O_{13}$ 978.5183; found 978.5149.

*(5S,10S,11S,18S)-18-Amino-11-benzyl-5-(tert-butyl)-19-methyl-3,6,13,17-tetraoxo-8-(4-(pyridin-2-yl)benzyl)-2,14,16-trioxa-4,7,8,12-tetraazaicosan-10-yl (S)-2-((methoxycarbonyl)amino)-3,3-dimethylbutanoate Dihydrochloride (**11**).* To the solid of (5*S*,10*S*,11*S*,18*S*)-11-benzyl-5-(*tert*-butyl)-18-isopropyl-22,22-dimethyl-3,6,13,17,20-pentaoxo-8-(4-(pyridin-2-yl)benzyl)-2,14,16,21-tetraoxa-4,7,8,12,19-pentaazatricosan-10-yl (*S*)-2-((methoxycarbonyl)amino)-3,3-dimethylbutanoate (**10**) (90 mg, 0.092 mmol) was added 4 N HCl in dioxane (0.5 mL, 2.00 mmol) at 0 °C under nitrogen atmosphere. After being stirred at 0 °C for 1 h, the reaction mixture was concentrated *in vacuo* at 30 °C. The residue was stirred with ether. The solvent was carefully decanted. The resultant solid was dried under vacuum to get the crude product as an off white solid. The solid was dissolved in a mixture of acetonitrile and water. The resulting mixture was frozen and lyophilized for 12.0 h to afford the title product as a white solid (67.33 mg; 76%). ^{1}H NMR (400 MHz, MeOH-d_4) δ 8.82 (d, J = 5.02 Hz, 1H), 8.58 (t, J = 7.65 Hz, 1H), 8.25−8.38 (m, 1H), 7.83−8.01 (m, 3H), 7.71 (d, J = 8.28 Hz, 2H), 7.54 (d, J = 9.54 Hz, 1H), 7.12−7.35 (m, 5H), 5.72−5.86 (m, 2H), 5.08 (br s, 1H), 4.60 (br s, 1H), 4.04−4.25 (m, 3H), 3.81−3.95 (m, 1H), 3.71 (s, 4H), 3.47−3.58 (m, 3H), 3.25 (dd, J = 7.28, 13.05 Hz, 1H), 3.06−3.18 (m, 1H), 2.89 (dd, J = 4.77, 13.80 Hz, 1H), 2.65−2.80 (m, 1H), 2.20 (qd, J = 6.90, 11.42 Hz, 1H), 1.08 (s, 9H), 0.93−1.03 (m, 6H), 0.81 (s, 9H); MS (ES): m/z 878.4 $[M+H]^+$. Analytical HPLC-RT and purity: method A = 6.415 min and 98.33%, method B = 7.754 min and 99.16%. HRMS (ESI/Orbitrap) m/z: $[M+H]^+$ calcd for $C_{45}H_{64}N_7O_{11}$ 878.4658; found 878.4648.

*(5S,10S,11S)-11-Benzyl-5-(tert-butyl)-15-chloro-16-methyl-3,6,13-trioxo-8-(4-(pyridin-2-yl)benzyl)-2,14-dioxa-4,7,8,12-tetraazaheptadecan-10-yl (2S)-2-((Methoxycarbonyl)amino)-3,3-dimethylbutanoate (**12**).* To a solution of (2*S*,3*S*)-3-amino-1-(2-((*S*)-2-((methoxycarbonyl)amino)-3,3-dimethylbutanoyl)-1-(4-(pyridin-2-yl)benzyl)hydrazinyl)-4-phenylbutan-2-yl (*S*)-2-((methoxycarbonyl)amino)-3,3-dimethylbutanoate dihydrochloride (**4**) (300 mg, 0.426 mmol) in anhydrous DCM (2 mL) were added pyridine (0.172 mL, 2.128 mmol) and 1-chloro-2-methylpropyl chloroformate (0.124 mL, 0.851 mmol) under nitrogen atmosphere. After being stirred at 0 °C for 3 h, the reaction mixture was partitioned between 1.5 N HCl and DCM. The organic layer was washed with water and brine, dried over anhydrous sodium sulfate, and concentrated under vacuum to get the crude product as a brown solid (320 mg, ∼90%). The crude product was found to be unstable for purification (CombiFlash/Prepartive HPLC) and hence was used as such in the next reaction. MS (ES): m/z 839.4 $[M+H]^+$

*(5S,10S,11S,18S)-11-Benzyl-5-(tert-butyl)-15,18-diisopropyl-22,22-dimethyl-3,6,13,17,20-pentaoxo-8-(4-(pyridin-2-yl)benzyl)-2,14,16,21-tetraoxa-4,7,8,12,19-pentaazatricosan-10-yl (2S)-2-((Methoxycarbonyl)amino)-3,3-dimethylbutanoate (**13**).* To a solution of (5*S*,10*S*,11*S*)-11-benzyl-5-(*tert*-butyl)-15-chloro-16-methyl-3,6,13-trioxo-8-(4-(pyridin-2-yl)benzyl)-2,14-dioxa-4,7,8,12-tetraaza-

DOI: 10.1021/acs.jmedchem.8b00277
J. Med. Chem. XXXX, XXX, XXX−XXX

heptadecan-10-yl (2*S*)-2-((methoxycarbonyl)amino)-3,3-dimethylbutanoate (**12**) (252 mg, 0.300 mmol) in DMF (1.0 mL) were added *N*-Boc-L-Val (98 mg, 0.450 mmol), DIPEA (0.262 mL, 1.501 mmol), and sodium iodide (45.0 mg, 0.300 mmol). The reaction mixture was heated at 50 °C for 14 h. The reaction mixture was diluted with water and extracted with EtOAc. The organic layer was washed with water and brine, dried over anhydrous sodium sulfate, and concentrated under vacuum to give the crude product. The crude product was purified by RP HPLC (Kinetex C18 (250 × 30 mm); mobile phase A: 10 mM ammonium acetate in water; mobile phase B: acetonitrile; flow rate: 20 mL/min.; gradient: 0/30, 10/70) to afford the title product (100 mg; 29.7%).^{1}H NMR (400 MHz, MeOH-d_4) δ 8.64−8.58 (m, 1H), 7.88 (d, J = 8.5 Hz, 4H), 7.58−7.50 (m, 2H), 7.40−7.33 (m, 1H), 7.30−7.14 (m, 5H), 6.52−6.39 (m, 1H), 5.12−5.04 (m, 1H), 4.58−4.46 (m, 1H), 4.23−4.03 (m, 3H), 4.02−3.89 (m, 1H), 3.71 (s, 4H), 3.52 (s, 3H), 3.30−3.23 (m, 1H), 3.16−3.00 (m, 1H), 2.89−2.81 (m, 1H), 2.78−2.63 (m, 1H), 2.10−1.90 (m, 2H), 1.42 (s, 9H), 1.08 (s, 9H), 0.96−0.85 (m, 12H), 0.79 (s, 9H); MS (ES): m/z 1020.4 $[M+H]^+$. Analytical HPLC-RT and purity: method B = 19.092 min and 98.1%; chiral HPLC-RT and purity: method A = 1.85 min and 95.1%, method B = 2.97 min and 100%. HRMS (ESI/Orbitrap) m/z: $[M+H]^+$ calcd for $C_{53}H_{78}N_7O_{13}$ 1020.5652; found 1020.5614.

*(5S,10S,11S,18S)-18-Amino-11-benzyl-5-(tert-butyl)-15-isopropyl-19-methyl-3,6,13,17-tetraoxo-8-(4-(pyridin-2-yl)benzyl)-2,14,16-trioxa-4,7,8,12-tetraazaicosan-10-yl (2S)-2-((methoxycarbonyl)-amino)-3,3-dimethylbutanoate Dihydrochloride (**14**).* To the solid of (5*S*,10*S*,11*S*,18*S*)-11-benzyl-5-(*tert*-butyl)-15,18-diisopropyl-22,22-dimethyl-3,6,13,17,20-pentaoxo-8-(4-(pyridin-2-yl)benzyl)-2,14,16,21-tetraoxa-4,7,8,12,19-pentaazatricosan-10-yl (2*S*)-2-((methoxycarbonyl)amino)-3,3-dimethylbutanoate (**13**) (90 mg, 0.088 mmol) was added 4 N HCl in dioxane (4.1 mL, 16.46 mmol) at 0 °C under nitrogen atmosphere. The reaction mixture was stirred at 0 °C for 1 h and subsequently concentrated *in vacuo* at 30 °C. The residue was stirred with ether, and the ether layer was decanted. The resultant solid was dried *in vacuo* to get crude product as an off-white solid. The solid was dissolved in a mixture of solvent acetonitrile and water. The resulting mixture was frozen and lyophilized for 12 h to afford the title product as a white solid (27.89 mg; 31.8%). ^{1}H NMR (400 MHz, MeOH-d_4) δ 8.78 (d, J = 5.02 Hz, 1H), 8.42−8.55 (m, 1H), 8.23 (d, J = 8.53 Hz, 1H), 7.86 (d, J = 8.53 Hz, 3H), 7.68 (d, J = 8.53 Hz, 2H), 7.50−7.35 (br s, 1H), 7.14−7.32 (m, 5H), 6.50 (d, J = 5.02 Hz, 1H), 5.08 (br s, 1H), 4.55 (br s, 1H), 4.08−4.24 (m, 3H), 3.94 (d, J = 4.02 Hz, 1H), 3.61−3.72 (m, 4H), 3.43−3.52 (m, 3H), 3.02−3.26 (m, 2H), 2.63−2.95 (m, 2H), 1.96−1.99(m 2H), 0.76−1.08 (m, 29H); MS (ES): m/z = 920.4 $[M+H]^+$. Analytical HPLC-RT and purity: method A = 7.21 min and 95.46%; method B = 8.16 min and 96.11%. HRMS (ESI/Orbitrap) m/z: $[M+H]^+$ calcd for $C_{48}H_{70}N_7O_{11}$ 920.5128; found 920.5097.

*(5S,10S,11S,18R)-11-Benzyl-5-(tert-butyl)-15,18-diisopropyl-22,22-dimethyl-3,6,13,17,20-pentaoxo-8-(4-(pyridin-2-yl)benzyl)-2,14,16,21-tetraoxa-4,7,8,12,19-pentaazatricosan-10-yl (2S)-2-((Methoxycarbonyl)amino)-3,3-dimethylbutanoate (**15**).* To a solution of (5*S*,10*S*,11*S*)-11-benzyl-5-(*tert*-butyl)-15-chloro-16-methyl-3,6,13-trioxo-8-(4-(pyridin-2-yl)benzyl)-2,14-dioxa-4,7,8,12-tetraazaheptadecan-10-yl (2*S*)-2-((methoxycarbonyl)amino)-3,3-dimethylbutanoate (**12**) (0.5 g, 0.453 mmol) in DMF (8.0 mL) was added *N*-Boc-D-Val (0.197 g, 0.905 mmol) followed by DIPEA (0.395 mL, 2.263 mmol) and sodium iodide (0.068 g, 0.453 mmol). The reaction mixture was heated at 60 °C for 8 h. The mixture was partitioned between ethyl acetate and water. The organic layer was concentrated under vacuum to give the residue, which was purified using RP- HPLC (preparative HPLC conditions: Sunfire C18 (150 × 19 mm; 5 μm), mobile phase A: 0.1% HCOOH in water, mobile phase B: acetonitrile, flow: 18 mL/min, gradient: 0/30, 10/80). The fraction was concentrated using high vacuum at 30 °C. The residue was dissolved in a mixture of acetonitrile and water. The resultant mixture was frozen and lyophilized for 12 h to get the title product (0.15 g, 0.144 mmol, 31.9% yield) as a white solid. ^{1}H NMR (400 MHz, MeOH-d_4) δ 8.61 (d, J = 4.0 Hz, 1H), 7.95−7.80 (m, 4H), 7.57−7.47 (m, 2H), 7.40−7.33 (m, 1H), 7.30−7.14 (m, 5H), 6.45 (d, J = 5.0 Hz, 1H), 5.10 (br s, 1H), 4.58 (br s, 1H), 4.23−4.13 (m, 2H), 4.10−3.95 (m, 2H), 3.71 (s, 3H), 3.66 (d, J = 2.5 Hz, 1H), 3.51 (s, 3H), 3.29−3.18 (m, 1H), 3.18−3.03 (m, 1H), 2.90−2.80 (m, 1H), 2.76−2.63 (m, 1H), 2.19−2.05 (m, 1H), 1.92 (dd, J = 12.5, 7.0 Hz, 1H), 1.50−1.37 (m, 9H), 1.08 (s, 9H), 0.98−0.85 (m, 12H), 0.81 (s, 9H); LCMS (ES): m/z 1020.4 $[M+H]^+$. Analytical HPLC-RT and purity: method B = 11.57 min and 99.34%; chiral HPLC-RT and purity: method A = 1.87 min and 97.1%, method B = 2.76 min and 97.3%. HRMS (ESI/Orbitrap) m/z: $[M+H]^+$ calcd for $C_{53}H_{78}N_7O_{13}$ 1020.5652; found 1020.5715.

*(5S,10S,11S,18R)-18-Amino-11-benzyl-5-(tert-butyl)-15-isopropyl-19-methyl-3,6,13,17-tetraoxo-8-(4-(pyridin-2-yl)benzyl)-2,14,16-trioxa-4,7,8,12-tetraazaicosan-10-yl (2S)-2-((Methoxycarbonyl)-amino)-3,3-dimethylbutanoate Dihydrochloride (**16**).* In a 5 mL round-bottom flask, (5*S*,10*S*,11*S*,18*R*)-11-benzyl-5-(*tert*-butyl)-15,18-diisopropyl-22,22-dimethyl-3,6,13,17,20-pentaoxo-8-(4-(pyridin-2-yl)-benzyl)-2,14,16,21-tetraoxa-4,7,8,12,19-pentaazatricosan-10-yl (2*S*)-2-((methoxycarbonyl)amino)-3,3-dimethylbutanoate (**15**) (0.04 g, 0.039 mmol) was taken and cooled to 0 °C. A solution of 4 M HCl in dioxane (2.47 mL, 9.87 mmol) was added, and the reaction mixture was stirred at 0 °C for 1 h. The mixture was then concentrated under vacuum. The residue was then triturated with ether, and the ether layer was decanted. The residue was dissolved in a mixture of acetonitrile and water. The resultant mixture was frozen and lyophilized for 12 h to get the title product (29.44 mg, 0.028 mmol, 71.5% yield) as a white solid. ^{1}H NMR (400 MHz, MeOH-d_4) δ 8.81 (d, J = 5.0 Hz, 1H), 8.61−8.51 (m, 1H), 8.29 (d, J = 8.0 Hz, 1H), 7.98−7.85 (m, 3H), 7.72 (d, J = 8.5 Hz, 2H), 7.35−7.17 (m, 5H), 6.46 (d, J = 4.5 Hz, 1H), 5.14 (d, J = 4.5 Hz, 1H), 4.52 (br s, 1H), 4.15 (s, 3H), 3.92 (d, J = 4.0 Hz, 1H), 3.70 (s, 3H), 3.59 (br s, 1H), 3.51 (s, 4H), 3.30−3.24 (m, 1H), 3.15 (br s, 1H), 2.91 (dd, J = 13.6, 4.5 Hz, 1H), 2.76−2.67 (m, 1H), 2.37−2.26 (m, 1H), 2.01 (d, J = 4.5 Hz, 1H), 1.15−1.03 (m, 15H), 0.99−0.90 (m, 6H), 0.81 (s, 9H); LCMS (ES): m/z 920.4 $[M+H]^+$. Analytical HPLC RT and purity: method A = 8.32 min and 94.81%; method B = 6.23 min and 94.53%. HRMS (ESI/Orbitrap) m/z: $[M+H]^+$ calcd for $C_{48}H_{70}N_7O_{11}$ 920.5128; found 920.5099.

■ ASSOCIATED CONTENT

Supporting Information

The Supporting Information is available free of charge on the ACS Publications website at DOI: 10.1021/acs.jmedchem.8b00277.

Details of *in vitro* and *in vivo* experiments (PDF)
Molecular formula strings (CSV)

■ AUTHOR INFORMATION

Corresponding Author

*Phone: +91-(0)9731600213. E-mail: murugaiah.andappan@syngeneintl.com or murugaiah.subbaiah123@gmail.com.

ORCID

Murugaiah A. M. Subbaiah: 0000-0001-5707-966X
Nicholas A. Meanwell: 0000-0002-8857-1515

Present Address

⊗For J.F.K., S.J., M.R.K., and C.W.: ViiV Healthcare, 36 East Industrial Road, Branford, CT 06405, USA

Notes

The authors declare no competing financial interest.

■ ACKNOWLEDGMENTS

We thank Drs. Arvind Mathur and Percy Carter for their support and inspiration. We especially acknowledge Dr. Sridhar Desikan for his guidance at the early stage of the program and Dr. Michael Sinz for critical review of the manuscript. We thank Drs. Punit Marathe, Michael Hageman, and Bruce Car for productive discussions. We acknowledge Dr. Arun Kumar

DOI: 10.1021/acs.jmedchem.8b00277
J. Med. Chem. XXXX, XXX, XXX−XXX

Gupta and team for an intermediate supply, the Discovery Analytical Sciences team for analytical support, and Dr. Sivaprasad Putlur for HRMS support.

■ ABBREVIATIONS USED

ATV, atazanavir; BLQ, below limit of quantification;; cART, combination antiretroviral therapy; DMAc, dimethylacetamide; FATP, fatty acid transport protein; HPβCD, hydroxypropyl β-cyclodextrin; PepT1, proton-coupled peptide transporter 1; PI, protease inhibitor; PPI, proton pump inhibitor; SMVT, sodium-dependent multivitamin transporter; SVCT, sodium-dependent vitamin C transporter; UGT1A1, uridine diphosphate glucuronosyltransferase 1A1

■ REFERENCES

(1) Zhan, P.; Pannecouque, C.; De Clercq, E.; Liu, X. Anti-HIV Drug Discovery and Development: Current Innovations and Future Trends. *J. Med. Chem.* **2016**, *59*, 2849−2878.

(2) Samji, H.; Cescon, A.; Hogg, R. S.; Modur, S. P.; Althoff, K. N.; Buchacz, K.; Burchell, A. N.; Cohen, M.; Gebo, K. A.; Gill, M. J.; Justice, A.; Kirk, G.; Klein, M. B.; Korthuis, P. T.; Martin, J.; Napravnik, S.; Rourke, S. B.; Sterling, T. R.; Silverberg, M. J.; Deeks, S.; Jacobson, L. P.; Bosch, R. J.; Kitahata, M. M.; Goedert, J. J.; Moore, R.; Gange, S. J. Closing the Gap: Increases in Life Expectancy Among Treated HIV-Positive Individuals in the United States and Canada. *PLoS One* **2013**, *8*, e81355.

(3) Ghosh, A. K.; Osswald, H. L.; Prato, G. Recent Progress in the Development of HIV-1 Protease Inhibitors for the Treatment of HIV/AIDS. *J. Med. Chem.* **2016**, *59*, 5172−5208.

(4) Midde, N. M.; Patters, B. J.; Rao, P.; Cory, T. J.; Kumar, S. Investigational Protease Inhibitors as Antiretroviral Therapies. *Expert Opin. Invest. Drugs* **2016**, *25*, 1189−1200.

(5) Farajallah, A.; Bunch, R. T.; Meanwell, N. A. Discovery and Development of Atazanavir. In *Antiviral Drugs*; John Wiley & Sons, Inc.: 2011; pp 1−17.

(6) *20th WHO Essential Medicines List (EML)*; World Health Organization (WHO), Geneva, 2017; http://www.who.int/medicines/publications/essentialmedicines/20th_EML2017_FINAL_amendedAug2017.pdf?ua=1 (accessed March 23, 2018).

(7) Appendix B, Table 3: *Characteristics of Protease Inhibitors*; https://aidsinfo.nih.gov/guidelines/htmltables/1/5482 (accessed March 23, 2018).

(8) Kis, O.; Zastre, J. A.; Hoque, M. T.; Walmsley, S. L.; Bendayan, R. Role of Drug Efflux and Uptake Transporters in Atazanavir Intestinal Permeability and Drug-Drug Interactions. *Pharm. Res.* **2013**, *30*, 1050−1064.

(9) Klein, C. E.; Chiu, Y. L.; Cai, Y.; Beck, K.; King, K. R.; Causemaker, S. J.; Doan, T.; Esslinger, H. U.; Podsadecki, T. J.; Hanna, G. J. Effects of Acid-Reducing Agents on the Pharmacokinetics of Lopinavir/Ritonavir and Ritonavir-Boosted Atazanavir. *J. Clin. Pharmacol.* **2008**, *48*, 553−562.

(10) Zhu, L.; Persson, A.; Mahnke, L.; Eley, T.; Li, T.; Xu, X.; Agarwala, S.; Dragone, J.; Bertz, R. Effect of Low-Dose Omeprazole (20 mg daily) on the Pharmacokinetics of Multiple-Dose Atazanavir with Ritonavir in Healthy Subjects. *J. Clin. Pharmacol.* **2011**, *51*, 368−377.

(11) Subbaiah, M. A. M.; Meanwell, N. A.; Kadow, J. F. Design Strategies in the Prodrugs of HIV-1 Protease Inhibitors to Improve the Pharmaceutical Properties. *Eur. J. Med. Chem.* **2017**, *139*, 865−883.

(12) Harbeson, S. L.; Tung, R. D. Azapeptide Derivatives. U.S. Patent 8,158,805, April 17, 2012.

(13) Clas, S. D.; Sanchez, R. I.; Nofsinger, R. Chemistry-Enabled Drug Delivery (Prodrugs): Recent Progress and Challenges. *Drug Discovery Today* **2014**, *19*, 79−87.

(14) Rautio, J.; Karkkainen, J.; Sloan, K. B. Prodrugs - Recent Approvals and a Glimpse of the Pipeline. *Eur. J. Pharm. Sci.* **2017**, *109*, 146−161.

(15) Vierling, P.; Greiner, J. Prodrugs of HIV protease inhibitors. *Curr. Pharm. Des.* **2003**, *9*, 1755−1770.

(16) Calogeropoulou, T.; Detsi, A.; Lekkas, E.; Koufaki, M. Strategies in the Design of Prodrugs of Anti-HIV Agents. *Curr. Top. Med. Chem.* **2003**, *3*, 1467−1495.

(17) Ouyang, H. Fosamprenavir: a Prodrug of Amprenavir. *Biotechnol.: Pharm. Aspects* **2007**, *5*, 541−549.

(18) DeGoey, D. A.; Grampovnik, D. J.; Flosi, W. J.; Marsh, K. C.; Wang, X. C.; Klein, L. L.; McDaniel, K. F.; Liu, Y.; Long, M. A.; Kati, W. M.; Molla, A.; Kempf, D. J. Water-Soluble Prodrugs of the Human Immunodeficiency Virus Protease Inhibitors Lopinavir and Ritonavir. *J. Med. Chem.* **2009**, *52*, 2964−2970.

(19) Patel, M.; Mandava, N.; Gokulgandhi, M.; Pal, D.; Mitra, A. K. Amino Acid Prodrugs: An Approach to Improve the Absorption of HIV-1 Protease Inhibitor, Lopinavir. *Pharmaceuticals* **2014**, *7*, 433−452.

(20) Wang, Z.; Pal, D.; Mitra, A. K. Stereoselective Evasion of P-Glycoprotein, Cytochrome P450 3A, and Hydrolases by Peptide Prodrug Modification of Saquinavir. *J. Pharm. Sci.* **2012**, *101*, 3199−3213.

(21) Gaucher, B.; Rouquayrol, M.; Roche, D.; Greiner, J.; Aubertin, A. M.; Vierling, P. Prodrugs of HIV Protease Inhibitors-Saquinavir, Indinavir and Nelfinavir-Derived from Diglycerides or Amino Acids: Synthesis, Stability and Anti-HIV Activity. *Org. Biomol. Chem.* **2004**, *2*, 345−357.

(22) De Kock, H. A.; Wigerinck, P. T. B. P.; Balzarini, J. Preparation of Peptidyl HIV Prodrugs Which are Cleavable by CD26. World Patent Application 2004/099135, Nov 18, 2004.

(23) Luo, S.; Wang, Z.; Patel, M.; Khurana, V.; Zhu, X.; Pal, D.; Mitra, A. K. Targeting SVCT for Enhanced Drug Absorption: Synthesis and In Vitro Evaluation of a Novel Vitamin C Conjugated Prodrug of Saquinavir. *Int. J. Pharm.* **2011**, *414*, 77−85.

(24) Luo, S.; Kansara, V. S.; Zhu, X.; Mandava, N. K.; Pal, D.; Mitra, A. K. Functional Characterization of Sodium-Dependent Multivitamin Transporter in MDCK-MDR1 Cells and its Utilization as a Target for Drug Delivery. *Mol. Pharmaceutics* **2006**, *3*, 329−339.

(25) Gerk, P. M.; Walsh, S. W.; Wang, M.; Landsberg, A. K. Prodrugs of HIV Protease Inhibitors Utilizing a Transporter-Directed Uptake Mechanism. U.S. Patent Appl. 20130267547, Oct 10, 2013.

(26) Skwarczynski, M.; Kiso, Y. Application of the O-N Intramolecular Acyl Migration Reaction in Medicinal Chemistry. *Curr. Med. Chem.* **2007**, *14*, 2813−2823.

(27) Hamada, Y.; Matsumoto, H.; Yamaguchi, S.; Kimura, T.; Hayashi, Y.; Kiso, Y. Water-Soluble Prodrugs of Dipeptide HIV Protease Inhibitors Based on O–>N Intramolecular Acyl Migration: Design, Synthesis and Kinetic Study. *Bioorg. Med. Chem.* **2004**, *12*, 159−170.

(28) Zhang, H.; Bonacorsi, S. J., Jr.; Chen, B.-C.; Leith, L. W.; Rinehart, J. K.; Balasubramanian, B.; Barrish, J. C. A Facile and Efficient Synthesis of d3-Labelled Reyataz. *J. Labelled Compd. Radiopharm.* **2005**, *48*, 1041−1047.

(29) Reddy, B. P.; Krishna, B. V.; Sharma, V. M.; Reddy, K. R.; Reddy, M. M. Preparation of Aza-Peptides Containing 2,2-Disubstituted Cyclobutyl and/or Substituted Alkoxybenzyl Derivatives as Antivirals. World Patent Application 2011/080562, July 7, 2011.

(30) Yanagisawa, H.; Koike, H.; Miura, S.-i. *Olmesartan Medoxomil: an Angiotensin II Receptor Blocker*; John Wiley & Sons, Inc.: 2012; pp 45−66.

(31) Hjermitslev, M.; Grimm, D. G.; Wehland, M.; Simonsen, U.; Krueger, M. Azilsartan Medoxomil, an Angiotensin II Receptor Antagonist for the Treatment of Hypertension. *Basic Clin. Pharmacol. Toxicol.* **2017**, *121*, 225−233.

(32) Giannarini, G.; Tascini, C.; Selli, C. Prulifloxacin: Clinical Studies of a Broad-Spectrum Quinolone Agent. *Future Microbiol.* **2009**, *4*, 13−24.

(33) Syed, Y. Y. Ceftobiprole Medocaril: A Review of Its Use in Patients with Hospital- or Community-Acquired Pneumonia. *Drugs* **2014**, *74*, 1523−1542.

DOI: 10.1021/acs.jmedchem.8b00277
J. Med. Chem. XXXX, XXX, XXX−XXX

(34) Alexander, J.; Bindra, D. S.; Glass, J. D.; Holahan, M. A.; Renyer, M. L.; Rork, G. S.; Sitko, G. R.; Stranieri, M. T.; Stupienski, R. F.; Veerapanane, H.; Cook, J. J. Investigation of (Oxodioxolenyl)methyl Carbamates as Nonchiral Bioreversible Prodrug Moieties for Chiral Amines. *J. Med. Chem.* **1996**, *39*, 480−486.
(35) Ishizuka, T.; Yoshigae, Y.; Murayama, N.; Izumi, T. Different Hydrolases Involved in Bioactivation of Prodrug-Type Angiotensin Receptor Blockers: Carboxymethylenebutenolidase and Carboxylesterase 1. *Drug Metab. Dispos.* **2013**, *41*, 1888−1895.
(36) Ishizuka, T.; Rozehnal, V.; Fischer, T.; Kato, A.; Endo, S.; Yoshigae, Y.; Kurihara, A.; Izumi, T. Interindividual Variability of Carboxymethylenebutenolidase Homolog, a Novel Olmesartan Medoxomil Hydrolase, in the Human Liver and Intestine. *Drug Metab. Dispos.* **2013**, *41*, 1156−1162.
(37) Ishizuka, T.; Fujimori, I.; Nishida, A.; Sakurai, H.; Yoshigae, Y.; Nakahara, K.; Kurihara, A.; Ikeda, T.; Izumi, T. Paraoxonase 1 as a Major Bioactivating Hydrolase for Olmesartan Medoxomil in Human Blood Circulation: Molecular Identification and Contribution to Plasma Metabolism. *Drug Metab. Dispos.* **2012**, *40*, 374−380.
(38) Poras, H.; Bonnard, E.; Dange, E.; Fournie-Zaluski, M.-C.; Roques, B. P. New Orally Active Dual Enkephalinase Inhibitors (DENKIs) for Central and Peripheral Pain Treatment. *J. Med. Chem.* **2014**, *57*, 5748−5763.
(39) Vig, B. S.; Huttunen, K. M.; Laine, K.; Rautio, J. Amino Acids as Promoieties in Prodrug Design and Development. *Adv. Drug Delivery Rev.* **2013**, *65*, 1370−1385.
(40) Krecmerova, M. Amino Acid Ester Prodrugs of Nucleoside and Nucleotide Antivirals. *Mini-Rev. Med. Chem.* **2017**, *17*, 818−833.
(41) Dhareshwar, S. S.; Stella, V. J. Your Prodrug Releases Formaldehyde: Should You be Concerned? No! *J. Pharm. Sci.* **2008**, *97*, 4184−4193.
(42) Hilfinger, J.; Shen, W. Preparation of Neuraminidase Inhibitor Analogs and Prodrugs, Especially Zanamivir and Oseltamivir Acid Analogs, with Enhanced Oral Bioavailability Useful in Treatment of Viral Infections, Particularly Influenza. World Patent Application 2011/123856, Oct 6, 2011.
(43) Mechanistic studies of this serendipitous discovery of diastereoselective *O*-alkylation are in progress.
(44) PubChem Website: *Isobutyraldehyde*; https://pubchem.ncbi.nlm.nih.gov/compound/isobutyraldehyde (accessed March 23, 2018).
(45) Petrillo, E. W. Case Study: Fosinopril. *Biotechnol.: Pharm. Aspects* **2007**, *5*, 551−558.
(46) Lal, R.; Sukbuntherng, J.; Tai, E. H. L.; Upadhyay, S.; Yao, F.; Warren, M. S.; Luo, W.; Bu, L.; Nguyen, S.; Zamora, J.; Peng, G.; Dias, T.; Bao, Y.; Ludwikow, M.; Phan, T.; Scheuerman, R. A.; Yan, H.; Gao, M.; Wu, Q. Q.; Annamalai, T.; Raillard, S. P.; Koller, K.; Gallop, M. A.; Cundy, K. C. Arbaclofen Placarbil, a Novel R-Baclofen Prodrug: Improved Absorption, Distribution, Metabolism, and Elimination Properties Compared with R-Baclofen. *J. Pharmacol. Exp. Ther.* **2009**, *330*, 911−921.
(47) Hoppe, E.; Hewitt, N. J.; Buchstaller, H. P.; Eggenweiler, H. M.; Sirrenberg, C.; Zimmermann, A.; Marz, J.; Schwartz, H.; Saal, C.; Meyring, M.; Hecht, S. A Novel Strategy for ADME Screening of Prodrugs: Combined Use of Serum and Hepatocytes to Integrate Bioactivation and Clearance, and Predict Exposure to Both Active and Prodrug to the Systemic Circulation. *J. Pharm. Sci.* **2014**, *103*, 1504−1514.
(48) Saxena, A.; Shah, D.; Padmanabhan, S.; Gautam, S. S.; Chowan, G. S.; Mandlekar, S.; Desikan, S. Prediction of pH Dependent Absorption Using In Vitro, In Silico, and In Vivo Rat Models: Early liability Assessment During Lead Optimization. *Eur. J. Pharm. Sci.* **2015**, *76*, 173−180.
(49) Zhang, L.; Wu, F.; Lee, S. C.; Zhao, H.; Zhang, L. pH-Dependent Drug-Drug Interactions for Weak Base Drugs: Potential Implications for New Drug Development. *Clin. Pharmacol. Ther. (N. Y., NY, U. S.)* **2014**, *96*, 266−277.

DOI: 10.1021/acs.jmedchem.8b00277
J. Med. Chem. XXXX, XXX, XXX−XXX